

BENDING OF CIRCULAR AND ANNULAR PLATES
ON MULTIPOINT SUPPORTS

by

Ramanath Williams

Thesis submitted to the Graduate Faculty of the
Virginia Polytechnic Institute and State University
in partial fulfillment of the requirements for the degree of
DOCTOR OF PHILOSOPHY
in
ENGINEERING MECHANICS

APPROVED:



H. F. Brinson, Chairman



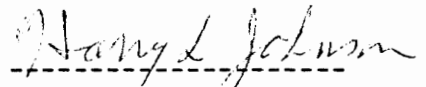
C. W. Smith



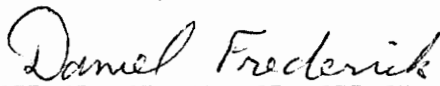
R. P. McNitt



R. J. Melosh



H. L. Johnson



D. Frederick, Department Head

January, 1974
Blacksburg, Virginia

LD
5655
Y856
1974
W55
c. 2

ACKNOWLEDGEMENTS

The author wishes to express his sincere appreciation to Dr. H. F. Brinson, his advisor, for his guidance and advice during the writing of this thesis and all through the author's graduate study. Also, the author wishes to thank his graduate advisory committee for showing interest and providing encouragement in writing this dissertation. Appreciation is also extended to Professor J. H. Sword for the time and effort he devoted to the development of computer programs used in this thesis. Finally, thanks must go to Mrs. Karen Matheson for typing this manuscript.

TABLE OF CONTENTS

SECTION	PAGE
List of Figures	iv
Notation.	vii
Introduction.	1
Literature Review	1
1.1 Circular Plate on Multipoint Supports	7
1.2 Comparison with Experimental Results.	18
1.3 Tables of Deflection Coefficients	20
1.4 Circular Plate on Multipoint Supports: Supports are Situated in Two Concentric Circles.	22
2. Annular Plate on Multipoint Supports.	29
References.	45
Figures	48
Appendix A.	81
Appendix B.	84

LIST OF FIGURES

Figure No.		Page No.
1	Symmetrically loaded circular plate on multipoint supports	51
2	System 1 in relation to Systems 2, 3 and 4	52
3	Circular plate on multipoint supports subjected to a concentrated force at center	53
4	Circular plate on multipoint supports subjected to a uniformly distributed load along a concentric ring	54
5	Uniformly loaded circular plate with multipoint supports	55
6	Details of the experimental specimen	56
7	Theoretical and experimental bending curves for the plate supported at different distances from its center	57
8	Theoretical and experimental bending deflection at the center of plate for supports at different distances from the center	58
9	Theoretical and experimental bending curves for the plate supported at three equally spaced points on its circumference	59
10	Curve showing the theoretical bending deflection at the point Q_1 , Q_2 and at the center for the plate (Fig. 6), for different s values	60

Figure No.		Page No.
11	Curve showing the maximum deviation in the theoretical bending deflection of the circular plate (Fig. 6) for different s values	61
12a	Uniformly loaded circular plate on multipoint supports	62
12b	Shaded portion of Figure 12a	62
13	Circular plate on multipoint supports; supports are situated in two support circles	63
14	Curve representing the deflection, w , of the plate shown in Figure 13	64
15	Contour map of plate shown in Figure 13	65
16	Uniformly loaded annular plate on multipoint supports	66
17	Schematic showing System 1 in relation to Systems 2, 3 and 4	67
18	Optimum position for least peak-to-peak deflection for a uniformly loaded annular plate on multipoint supports	68
19	Optimized peak-to-peak deflection vs. hole size for a uniformly loaded annular plate on multipoint supports	69
20	Contour map of uniformly loaded annular plate on three equally spaced point supports which are not at the optimum positions	70

Figure No.

Page No.

21 Contour map of uniformly loaded annular
plate with three equally spaced point
supports at the optimum positions

71

NOTATION

a	radius of inner circle for annular plate
b	radius of support circle for single support circle
c	radius of plate
D	flexural rigidity of plate, $D = Eh^3/12(1-\nu^2)$
d	radius of loading circle
E	modulus of elasticity
h	uniform plate thickness
K	$Wc^2/8\pi D$
\bar{K}	$qc^4/8D$
N	number of supports
p	a/c
q	uniform load intensity
(r,θ)	polar coordinates
s	b/c
t	d/c
T	number of supports, applies only to plate with two support circle
W	total load on plate
x	r/c
α	angle between supports, $\alpha = 2\pi/N$
β	deflection coefficient for circular plate
δ	off-set angle, applies only to plate with two support circle
λ	$(3+\nu)/(\nu-1)$
ν	Poisson's ratio

M_{ri}	radial bending moment	}	(i=1,2,3,4)
V_i	reaction		
w_i	deflections		

INTRODUCTION

The purpose of the present investigation is to determine the deflection surface of circular and annular plates supported on multipoint supports; and then from the derived analytical surface, study the influence of support circle diameter and the size of the hole for any given number of concentrated force supports and thus predict suitable analytical criterion for minimum deflection of plates.

The above class of problems frequently occurs in structural engineering; for example, the offshore platforms, as well as the floor system of high-rise buildings which are supported essentially by columns. The results and conclusions to be derived in this dissertation would also be of value in optical engineering, where optical mirrors are designed for least deflection, while the lens and its support structures are subjected to minimum weight. The latter requirement is often achieved by introducing concentrated supports rather than continuous supports.

LITERATURE REVIEW

The problems to be investigated in the dissertation are generally called "Concentrated Force Problems in Transverse Bending of Plates." A historical literature survey on this topic will now be given.

The solution corresponding to a rigidly clamped circular plate under a concentrated load at the center was first obtained by Poisson (1) in (1829). Clebsch (2) in (1862) was the first to formulate the problem of a clamped circular plate subjected to a concentrated force at an arbitrary point. Slight errors in the complex computation of this

problem were later corrected by Foeppel (3). Clebsch's solution did not, however, contain the concentrated load singularity in closed form.

Michell (4) has the merit to simplify the Clebsch's problem by using the process of inversion--which leads to the solution for an eccentric load by the inversion of that for a centrally loaded circular plate. Mathematically, Michell found a closed form expression for the "Green's function" for the differential equation $\nabla^4 w = 0$ within a circular boundary. Twenty years later Melan (5) recovered the same solution by use of bipolar coordinates.

At present there are a number of solutions to various types of problems on bending of plates subjected to concentrated forces. Most of these problems are approached by means of the complex variable method of Muskhelishvili, which was extended to plate bending problems by Lechnitskii (6).

Lurie (7) applied the Muskhelishvili-Lechnitskii method for solving the biharmonic equation and discussed several problems in the bending of circular plates. Friedmann (8) considered the problem of the bending of a thin isotropic plate when acted upon by any number of normal concentrated forces at interior or boundary points. Applying the complex variable method, Chankvetadze (9) found a solution in closed form for a thin circular plate normally and uniformly loaded over the whole plate and supported at a number of points on its periphery. The same method was used by Washizu (10) to discuss the bending of a circular plate under several concentrated loads on the boundary, the faces of the plate being free from normal forces. The boundary condition taken by Washizu is of a form different from that used by Friedmann and Chankvetadze, and may

be obtained from it by differentiation.

In Reference (11) Yi-Yuan Yu studied the bending of isotropic homogeneous thin plates, the boundaries of which were subjected to isolated couples and forces. An excellent paper by Bassali (12) considers the problem of a thin circular plate supported at several interior or boundary points and transversely loaded over the area of an eccentric circle. This latter problem is formulated and solved in great generality by means of complex variables; therefore, it would require considerable amount of analysis prior to its engineering application.

Nadai (13), without making use of complex variables, gave a general method for handling problems of circular plates symmetrically loaded with respect to the center and supported at several points along the boundary. The method of Nadai is also outlined by Timoshenko and Woinowsky-Krieger (14). The same method was used by DeBeer (15) to obtain the deflection at any point of a symmetrically loaded circular plate supported in a number of points regularly distributed around the boundary. Following similar reasoning and using the superposition principle, Bassali (16) found infinite series solutions for circular plates subjected to certain loadings over the area of an eccentric circle, where the plate is supported at several points along the boundary. In another paper by Yu and Pan (17) a circular plate supported on symmetrical points located along a concentric interior circle was investigated. Leissa and Wells (18), by means of a Fourier series in real variables, have also found a solution to a uniformly loaded circular plate having two, four and eight symmetrically located interior point supports. By extending the method of Nadai (13), mentioned above, the solution for the circular plate

plate supported by uniformly distributed reactions over finite arcs of the boundary is given by Girkmann (19). Reismann (20) investigated the effect of an elastic boundary restraint upon the deflection, moments and critical buckling loads of a circular plate while the plate is subjected to a concentrated force at an arbitrary point.

All of the above discussion on literature survey are for circular plates. As regards annular plates, there are only a few known solutions when the plate is under the action of concentrated forces. Symonds (21), by means of inversion, has found a closed form solution of the problem of an infinitely large plate clamped at an inner circular edge, with outer edge free, and loaded by a concentrated force at an arbitrary point. From this result, Symonds also finds an infinite series solution to a ring shaped plate of finite outer radius, with force applied either at the outer edge or at any point between the inner clamped edge and the outer edge. The first case, in which the force is applied at the outer boundary was originally solved by H. Reissner (22). In another paper, Amon and Widera (23) outlined the procedure for handling an annular plate clamped at both inner and outer boundaries and loaded by a concentrated force. The bending by uniform load of an annular plate supported at one or both of the circular edges on equally spaced columns is considered by Agabain, Lee and Dandurs (24).

Having discussed the available solutions to bending problems in the presence of concentrated forces, the contents of the dissertation will now be given.

CONTENT OF DISSERTATION

1.1 Explicit formulae are to be derived for the deflection surface of a symmetrically loaded circular plate having several point supports which are situated at equal distances apart on a single concentric circle, which may be as large as the diameter of the plate itself.

1.2 Compare the derived results, which would be exact in accordance with classical thin plate theory, with the experimental data given by Emerson (25) and Dew (26).

1.3 Provide numerical deflection coefficients for a uniformly loaded circular plate; this information could be utilized for optimizing the position and the number of supports.

1.4 Provide a numerical method which would give deflection surface for a uniformly loaded circular plate which is point supported, but has two support circles; the supports being all in the same level.

2. Derive the expression for the deflection surface of a uniformly loaded annular plate having any number of point supports which are situated at equal distances apart on any single concentric circle; and from this result, determine the optimum position for support circle for a given size of hole and the number of supports.

METHOD OF SOLUTION TO PLATES ON MULTIPPOINT SUPPORTS

In the presence of concentrated forces, solutions to plate bending problems are complicated. However, as was illustrated by Bassali (12), these types of problems can be systematically and successfully solved by means of the complex variable method. Unfortunately, the solutions

that are available by this method are too general and the final results given by the authors are in terms of functions of complex variables. Because of this reason, it would require further mathematical analysis to adapt the solution to a physical problem--or to extend the analysis and solution to some other related problem.

Of course, there are a number of solutions to plate bending problems in the presence of concentrated forces, which are approached in terms of functions of real variables. Solutions available in terms of real variables are, however, restricted to cases where the support points are along the boundary: The reason for this limitation is due to the following fact. When the support points are anywhere other than the boundary, the problem has to be approached by means of the method suggested by Clebsch (2), and this method is also given in page 290 of Reference (14): The solution obtained by the Clebsch method would be in terms of infinite series, and as was shown by Yu and Pan (17), the solution consists of two parts; one for the region interior to the support circle and the other for the region exterior to the support circle. A general difficulty of this method is due to the slow convergence of the series in the neighborhood of the supports, which makes numerical evaluation tedious if not impossible. However, when the supports are at the boundary, the problem is relatively easy and can be solved by the method suggested by Nadai (13): This method is also given in page 293 of Reference (14). Nadai's method also gives an infinite series solution, but the series converges much more rapidly.

In the following pages, a method will be given to derive the deflection surface of a symmetrically loaded circular plate having several

point supports which are situated equal distances apart on a single concentric circle. There is no restriction on the diameter of the support circle, which may be as large as the diameter of the plate itself. The approach to the problem here is essentially superposition of relevant known solutions. In particular, the singularity effects associated with the concentrated supports on the plate are accounted for by considering the solution obtained by Michell (4) for a clamped circular plate subjected to an eccentric point load. The approach to annular plate on multipoint supports is similar to that of a circular plate.

1.1 CIRCULAR PLATE ON MULTIPOINT SUPPORT

STATEMENT OF PROBLEM

The problem to be investigated consists of determining the deflection surface of a constant thickness circular plate of radius c subjected to the following three conditions:

1. The total load W is symmetrically distributed with respect to the center of the plate.
2. The plate is supported by N ($N \geq 2$) concentrated forces, each of magnitude (W/N) , and located equal distances apart on a single concentric circle of radius b .
3. The plate has the boundary conditions of a free edge.

The circular plate with the above specified conditions, illustrated in Figure 1, will be referred to as System 1. The loading and support conditions on the plate of System 1 are such that, the equilibrium of forces and moments are satisfied.

METHOD AND SOLUTION

The solution to the above problem will now be found on the basis of classical small-deflection theory. According to this theory, the transverse deflections w_1 of System 1 are characterized by

$$\nabla^4 w_1 = q(r)/D \quad (1)$$

where D is the flexural rigidity and $q(r)$ is the axi-symmetric load intensity, which is related to the total load W by

$$W = 2\pi \int_0^c q(r) r dr \quad (2)$$

In view of the conditions on System 1, it will be assumed that the deflections w_1 are of the form

$$w_1 = w_2 + w_3 + w_4 \quad (3)$$

such that, w_2 , w_3 and w_4 correspond respectively to deflections of the following three systems. The boundary, loading and the support conditions of these three systems are illustrated in relation to System 1 in Figure 2.

System 2: This system is a simply supported circular plate of radius c subjected to the same type of loading as the plate of System 1.

System 3: The effects of concentrated supports on the plate of System 1 are accounted for by defining System 3 as a clamped circular plate of radius c , subjected to a loading condition which is identical to the support condition of System 1.

The deflections, bending moments and edge reactions corresponding to Systems 2 and 3 are obtainable from Reference (14); however, for

reference purposes, relevent data on Systems 2 and 3 are given in Appendix A.

System 4: This system consists of a circular plate of radius c which is not subjected to any surface loading but has applied moment and reaction distributions along the periphery. These distributions are such that the total moment and reaction at the boundary of Systems 2, 3, and 4 are zero.

The deflection surface w_4 corresponding to System 4 will now be found on the reasoning that the System 1 has the boundary conditions of a free edge. By Kirchhoff's theory of plates, the boundary conditions of a free edge for the plate of System 1 are characterized by

$$(M_{r1})_{r=c} = -D \left[\nabla^2 w_1 + \frac{(1-\nu)}{c^2} \frac{\partial^2 w_1}{\partial x^2} \right]_{x=1} = 0 \quad (4)$$

since there is no bending moment along a free edge.

$$(V_1)_{r=c} = -D \left[\frac{1}{c} \frac{\partial \nabla^2 w_1}{\partial x} + \frac{(1-\nu)}{c^3 x} \frac{\partial^2}{\partial x \partial \theta} \left\{ \frac{1}{x} \frac{\partial w_1}{\partial \theta} \right\} \right]_{x=1} = 0 \quad (5)$$

Since there is no edge reaction for a free edge,

where,

$$\left. \begin{aligned} & x = r/c \\ \text{and,} & \end{aligned} \right\} \quad (6)$$

$$\nabla^2 = \frac{1}{c^2} \left[\frac{\partial^2}{\partial x^2} + \frac{1}{x} \frac{\partial}{\partial x} + \frac{1}{x^2} \frac{\partial^2}{\partial \theta^2} \right]$$

Substituting equation (3) in equation (4) gives

$$-(M_{r4})_{r=c} = (M_{r2})_{r=c} + (M_{r3})_{r=c} \quad (7)$$

where

$(M_{r2})_{r=c}$ and $(M_{r3})_{r=c}$ are given by equations (A2) and (A7) respectively, and

$$(M_{r4})_{r=c} = -D \left[\nabla^2 w_4 + \frac{(1-\nu)}{c^2} \frac{\partial^2 w_4}{\partial x^2} \right]_{x=1} \quad (8)$$

Substituting equations (A2), (A7) in equation (7) yields

$$(M_{r4})_{r=c} = - \frac{W(1-s^2)}{2\pi} \left[\frac{1}{2} + \frac{1}{N} \sum_{n=1}^N \sum_{m=2}^{\infty} s^m \cos m(\theta-n\alpha) \right] \quad (9)$$

Substituting (3) in equation (5) gives

$$-(V_4)_{r=c} = (V_2)_{r=c} + (V_3)_{r=c} \quad (10)$$

where,

$(V_2)_{r=c}$ and $(V_3)_{r=c}$ are given respectively by equations (A3) and (A8), and

$$(V_4)_{r=c} = -D \left[\frac{1}{c} \frac{\partial \nabla^2 w_4}{\partial x} + \frac{(1-\nu)}{c^3} \frac{\partial^2}{\partial x \partial \theta} \left\{ \frac{1}{x} \frac{\partial w_4}{\partial \theta} \right\} \right]_{x=1} \quad (11)$$

Substituting equations (A3), (A8) in equation (10) yields

$$(V_4)_{r=c} = - \frac{W}{2\pi Nc} \sum_{n=1}^N \sum_{m=2}^{\infty} \left(2 + m(1-s^2) \right) s^m \cos m(\theta-n\alpha) \quad (12)$$

The form of the boundary values for System 4, given by equations (9) and (12) suggests that deflections w_4 are of the form

$$w_4 = A + B x^2 + \sum_{n=1}^N \sum_{m=2}^{\infty} (A_m + B_m x^2) x^m s^m \cos m(\theta-n\alpha) \quad (13)$$

If equation (13) is substituted in equations (9) and (12), it can be shown that

$$\left. \begin{aligned}
 B &= \frac{Wc^2 (1-s^2)}{8\pi D (1+v)} \\
 A_m &= \frac{Wc^2}{2\pi N D (3+v)} \left[\frac{s^2}{m} - \frac{2(1+v)}{m^2 (m-1) (1-v)} - \frac{1}{(m-1)} \right] \\
 B_m &= \frac{Wc^2}{2\pi N D (3+v)} \left[\frac{1}{m} - \frac{s^2}{(m+1)} \right]
 \end{aligned} \right\} \quad (14)$$

By substituting equation (14) in equation (13), w_4 becomes

$$\begin{aligned}
 w_4 &= A + \frac{Wc^2 (1-s^2)}{8\pi D (1+v)} x^2 + \frac{Wc^2 (x^2+s^2)}{2\pi N D (3+v)} \sum_{n=1}^N \sum_{m=2}^{\infty} \frac{x^m s^m}{m} \cos m(\theta-n\alpha) \\
 &\quad - \frac{Wc^2}{2\pi N D (3+v)} \sum_{n=1}^N \sum_{m=2}^{\infty} \left[\frac{1}{(m-1)} + \frac{s^2 x^2}{(m-1)} \right] x^m s^m \cos m(\theta-n\alpha) \\
 &\quad - \frac{Wc^2 (1+v)}{\pi N D (1-v) (3+v)} \sum_{n=1}^N \sum_{m=2}^{\infty} \frac{x^m s^m}{m^2 (m-1)} \cos m(\theta-n\alpha) \quad (15)
 \end{aligned}$$

Substituting equations (B1), (B4) and (B5) of Appendix B in the above equation yields

$$w_4 = A + w_4^* \quad (16)$$

where,

$$\begin{aligned}
 w_4^* &= \frac{Wc^2}{\pi D} \left\{ \frac{(1-s^2) x^2}{8 (1+v)} + \frac{s^2 x^2}{2(3+v)} \right. \\
 &\quad - \frac{(1+v)}{(3+v) (1-v)} \sum_{m=N, 2N, \dots}^{\infty} \frac{x^m s^m \cos m\theta}{m^2 (m-1)} - \frac{1}{4\pi N (3+v)} \sum_{n=1}^N [x^2 + s^2 - 2xs \cos(\theta-n\alpha)] \\
 &\quad \left. \times \log [1 + x^2 s^2 - 2xs \cos(\theta-n\alpha)] \right\} \quad (17)
 \end{aligned}$$

By substituting equation (16) in equation (3), the constant A can be evaluated using the conditions that the deflections w_1 are zero at

the support points, and that w_1 are periodic with a period of $\alpha = 2\pi/N$; thus

$$A = -[w_2 + w_3 + w_4^*]_{x=s, \theta=0} \quad (18)$$

On substituting equations (16) and (A6) in equation (3), and using equations (17 and (18), it can be shown that the deflections w_1 are of the form

$$w_1 = w_2 - [w_2]_{x=s} + \Phi(x, \theta) \quad (19)$$

where

$$\begin{aligned} \Phi(x, \theta) = & \frac{K(\lambda^2 - s^2)(x^2 - s^2)}{\lambda(\lambda+1)} + \frac{Ks^2}{N\lambda} \sum_{n=1}^{N-1} (1 - \cos n\alpha) \log \left[\frac{[2s^2(1 - \cos n\alpha)]^\lambda}{1 + s^4 - 2s^2 \cos n\alpha} \right] \\ & + \frac{K}{2N\lambda} \sum_{n=1}^N [x^2 + s^2 - 2xs \cos(\theta - n\alpha)] \log \left[\frac{1 + x^2 s^2 - 2xs \cos(\theta - n\alpha)}{[x^2 + s^2 - 2xs \cos(\theta - n\alpha)]^\lambda} \right] \\ & + \left[K \frac{(\lambda^2 - 1)}{\lambda} \sum_{m=N, 2N, \dots}^{\infty} \frac{x^m s^m}{m^2 (m-1)} \cos m\theta \right] - \left[K \frac{(\lambda^2 - 1)}{\lambda} \sum_{m=N, 2N, \dots}^{\infty} \frac{s^{2m}}{m^2 (m-1)} \right] \end{aligned} \quad (20)$$

where,

$$K = \frac{Wc^2}{8\pi D} \quad \text{and} \quad \lambda = \frac{(3+\nu)}{(\nu-1)} \quad (21)$$

By using equations (B14) and (B17) of Appendix B, it can be shown that equation (19) is in agreement with Bassali's result (12). Although Bassali's results are compact in form, it must be realized that they are expressed in terms of complex quantities. For practical numerical problems, it would be convenient to express the deflections w_1 in terms of real quantities, as in equations (19) and (20). The application of these two equations to practical problems may be illustrated considering

the following examples.

EXAMPLE 1. Circular plate subjected to symmetrical loading and supported by N point forces which are situated at equal distances apart on the circumference of the plate.

For this problem $s=1$. Since the deflections w_2 correspond to a simply supported plate, it follows that they vanish along the edge of the plate; that is, $(w_2)_{x=s=1} = 0$. Therefore from equations (19) and (20)

$$\begin{aligned} \lim_{s \rightarrow 1} (w_1) &= w_2 + \frac{K(\lambda-1)}{\lambda} (x^2-1) + \frac{K(\lambda^2-1)}{\lambda} \sum_{m=N, 2N, \dots}^{\infty} \frac{(x^m \cos m\theta - 1)}{m^2(m-1)} \\ &+ \frac{K(1-\lambda)}{2N\lambda} \sum_{n=1}^N [1+x^2-2x \cos(\theta-n\alpha)] \log [1+x^2-2x \cos(\theta-n\alpha)] \\ &+ \frac{K(\lambda-1)}{N\lambda} \sum_{n=1}^{N-1} (1-\cos n\alpha) \log [2(1-\cos n\alpha)] \end{aligned} \quad (22)$$

Using equations (B7) it can be shown that

$$\begin{aligned} \lim_{s \rightarrow 1} (w_1) &= w_2 - \frac{K(\lambda-1)}{\lambda} \sum_{m=N, 2N, \dots}^{\infty} \left[\frac{1}{m(m-1)} - \frac{(\lambda+1)}{m^2(m-1)} - \frac{x^2}{m(m+1)} \right] x^m \cos m\theta \\ &+ \frac{K(\lambda-1)}{\lambda} \sum_{m=N, 2N, \dots}^{\infty} \left[\frac{2}{m(m^2-1)} - \frac{(\lambda+1)}{m^2(m-1)} \right] \end{aligned} \quad (23)$$

Equation (23) is the general expression for the deflection surface of a circular plate of radius c , subjected to a symmetrical loading and supported by equally spaced point loads along the edge of the plate.

This result was originally derived by Nadai (13) by a different method and the derivation procedure is also given in Reference (14).

EXAMPLE 2. Circular plate of radius c , is subjected to a concentrated force W at the center: The plate is supported at equal distances apart

on a concentric circle of radius b by concentrated forces (Figure 3).

With reference to equation (19), the deflections w_2 for this example corresponds to a simply supported circular plate of radius c subjected to a point load W at the center of the plate; thus, from Reference (14), these deflections are given by,

$$w_2 = \frac{K}{2} \left[\frac{3+\nu}{1+\nu} (1+x^2) + 2x^2 \log x \right] \quad (24)$$

therefore

$$w_2(x=s) = \frac{K}{2} \left[\frac{3+\nu}{1+\nu} (1+s^2) + 2s^2 \log s \right] \quad (25)$$

Substituting equations (24) and (25) in equation (19) yields,

$$w_1 = \frac{K}{2} \left[\frac{3+\nu}{1+\nu} (s^2 - x^2) + 2(x^2 \log x - s^2 \log s) \right] + \phi(x, \theta) \quad (26)$$

where, $\phi(x, \theta)$ is defined by equation (20).

The central deflection corresponding to this example obtained by substituting $x = 0$ in equation (26); thus,

$$\begin{aligned} w_1(x=0) &= \frac{K}{2} \left[\frac{3+\nu}{1+\nu} s^2 - 2s^2 \log s \right] + K s^2 \log s - K \frac{(\lambda^2 - s^2)}{\lambda(\lambda+1)} s^2 \\ &+ \frac{Ks^2}{N\lambda} \sum_{n=1}^{N-1} (1 - \cos n) \log \frac{[2s^2 (1 - \cos n\alpha)]^\lambda}{(1+s^4 - 2s^2 \cos n\alpha)} \\ &+ K \frac{(\lambda-1)}{\lambda} \sum_{m=N, 2N, \dots}^{\infty} \frac{s^{2m}}{m^{2(m-1)}} \end{aligned} \quad (27)$$

The formulae corresponding to central deflection of a circular plate loaded at center by a concentrated force W and supported by six point forces at the circumference of the plate will now be derived.

Substituting $s=1$ in equation (27) then using equation (B22) and

the relation,

$$(1 - \cos n\alpha) = 2 \sin^2 n\alpha/2$$

gives the following expression for the central deflection

$$w_1(x=0) = \frac{K}{\lambda(\lambda+1)} - K \frac{(\lambda-1)^2}{3\lambda} \sum_{n=1}^5 \sin^2 \frac{n\alpha}{2} \log (2 \sin n\alpha/2) \\ + K \frac{(\lambda^2-1)}{\lambda} \left[\frac{\pi^2}{216} - \frac{1}{12} \sum_{n=1}^5 (\pi-n\alpha) \sin n\alpha \right]$$

The above equation may be simplified, to give

$$w_1(x=0) = \frac{K}{\lambda} \left[\frac{1}{(\lambda+1)} - \frac{(\lambda-1)^2}{3} \left(\frac{3}{4} \log 3 + \log 2 \right) + (\lambda^2-1) \frac{\pi^2}{216} \right] \quad (28)$$

EXAMPLE 3. A circular plate of radius c is supported at N equally spaced points on a concentric circle of radius b and it is subjected to a total load W , which is uniformly distributed along a concentric circle of radius d , such that $b > d$. (Figure 4)

The deflections w_2 for this example consists of two parts; these are given by (Reference (14), page 64) for the inner portion of the plate (i.e., $0 \leq r \leq d$)

$$w_2 = K \left[\frac{(1-t^2)}{2} \left\{ \frac{3+\nu}{1+\nu} - \left(\frac{1-\nu}{1+\nu} \right) x^2 \right\} + (t^2 + x^2) \log t \right] \quad (29)$$

and for the outer portion of the plate (i.e., $d \leq r \leq c$)

$$w_2 = K \left[\frac{(1-x^2)}{2} \left\{ \frac{3+\nu}{1+\nu} - \left(\frac{1-\nu}{1+\nu} \right) t^2 \right\} + (t^2 + x^2) \log x \right] \quad (30)$$

in which,

$$t = d/c; \quad x = r/c$$

With reference to equation (19), the quantity $[w_2]_{x=s}$, must be such

such that, the deflections w_1 vanish at the support points. Since the support circle is larger than the loading circle, it follows that the support points are at the outer portion of the plate, and therefore, for w_1 to be zero at the support points $[w_2]_{x=s}$ has to be found from equation (30). Thus,

$$[w_2]_{x=s} = K \left[\frac{(1-s^2)}{2} \left\{ \frac{3+\nu}{1+\nu} - \frac{(1-\nu)}{1+\nu} \right\} t^2 \right] + (t^2 + s^2) \log s \quad (31)$$

The deflections w_1 for the plate, shown in Figure 4, consist of two parts: One of which is for the outer portion of the plate, and the other for the inner portion of the plate.

The deflections for the outer part ($d \leq r \leq c$) are obtained by substituting equations (30) and (31) in equation (19). If the deflections are required for the inner portion ($0 \leq r \leq d$) then equation (29) must be used instead of equation (30).

EXAMPLE 4. A circular plate of radius c is subjected to a uniform load and supported on a concentric circle of radius b by point forces. (Figure 5).

With reference to equation (19), the deflections w_2 for this example corresponds to a simply supported circular plate of radius c subjected to a uniformly distributed load. In this case the deflections w_2 are given by (page 57, Reference 14).

$$w_2 = \frac{K(1-x^2)}{8} \left[\frac{(5+\nu)}{(1+\nu)} - x^2 \right] \quad (32)$$

therefore,

$$[w_2]_{x=s} = \frac{K(1-s^2)}{8} \left[\frac{(5+\nu)}{(1+\nu)} - s^2 \right] \quad (33)$$

substituting equations (32) and (33) in equation (19), and using equation (20) yields,

$$\begin{aligned}
 w_1 = & \frac{K}{2N\lambda} \sum_{n=1}^N (x^2 + s^2 - 2xs \cos (\theta - n\alpha)) \log \left[\frac{1+x^2 s^2 - 2xs \cos (\theta - n\alpha)}{[x^2 + s^2 - 2xs \cos (\theta - n\alpha)]^\lambda} \right] \\
 & + \frac{2Ks^2}{N\lambda} \sum_{n=1}^{N-1} (\sin^2 n\alpha/2) \log \left[\frac{[2s \sin n\alpha/2]^{2\lambda}}{(1+s^4 - 2s^2 \cos n\alpha)} \right] \\
 & + \frac{K(\lambda^2 - 1)}{\lambda} \left(\sum_{m=N, 2N, \dots}^{\infty} \left[\frac{x^m s^m \cos m\theta}{m^2 (m-1)} \right] - \sum_{m=N, 2N, \dots}^{\infty} \left[\frac{s^{2m}}{m^2 (m-1)} \right] \right) \\
 & + \frac{K(x^4 - s^4)}{8} + \frac{K(\lambda^2 - 2s^2)}{2\lambda(\lambda+1)} (x^2 - s^2) \tag{34}
 \end{aligned}$$

where,

$$K = \frac{Wc^2}{8\pi D} = \frac{qc^4}{8D}$$

in which q is the uniform load intensity.

1.2 COMPARISON WITH EXPERIMENTAL RESULTS

In his article, "Determination of Planeness and Bending of Optical Flats," Emerson (25) has given some valuable information regarding the determination of bending deflections from experiments. His experimental self weight deflection curves are compared herein with the theoretical deflection curves which are obtained using equation (34).

The experimental specimen used by Emerson was an optical flat of fused quartz: Relevant dimensions and physical properties of the test specimen are given in Figure 6. The theoretical self weight deflection curves shown in Figures 7, 8 and 9, were obtained by substituting the constants provided by Emerson in equation (34). The total distributed loading on the plate is assumed equal to the weight of the plate.

The deflection surfaces shown in Figures 7, 8 and 9, are given relative to the points P and P_1 of Figure 6 instead of the more usual practice of giving deflections relative to plane of supports. This permits direct comparison between the accuracy of the theoretical results and the experimental results obtained and presented in this form by Emerson.

It was found by Emerson that, if the circular flats were supported at 0.7 of the radius of the plate, then the bending deflections would be quite small. Considering that he measures the deflections only along a single line (i.e., the line joining the points P and P_1 of Figure 6), one could debate on the suggested support position for the overall least sag. In examining Emerson's results, Dew (26) remarks that the overall least sag for the three point support of optical flats

can be achieved by supporting them at 0.6 of the radius of the flat, rather than 0.7 as suggested by Emerson.

As there is no definite answer as regards the suitable position for supports by experimental means, it was decided to utilize equation (34) to conclude upon a support circle radius which yields least overall sag.

Figure 10 shows the theoretical deflections at the points Q_1 , Q_2 and the center of the flat (shown in Figure 6) when it is supported at different distances from the center of the flat. The deflections shown in this figure are relative to the plane of the supports. The reason for considering the deflections at these three positions is that the deflections at any location of the flat would be bounded by the deflections occurring at any two points of the above mentioned three locations.

The maximum deviation in deflections, i.e., the maximum peak-to-peak deflections, are calculated from the numerical data of Figure 10. These deviations in deflections are shown with respect to various support positions in Figure 11.

It can be seen from this latter figure, that the least overall sag for a circular plate with three equally spaced point supports occurs when the support circle radius is 0.66 of the radius of the plate.

1.3 TABLES OF DEFLECTION COEFFICIENTS

The deflection surface w_1 corresponding to a circular plate of constant thickness, subjected to uniform pressure over the entire plate and having N symmetrical point supports is defined by equation (34). However, manipulation of this equation to select the optimum number and position of supports would constitute a lengthy process. For this reason, numerical deflection coefficients are provided here, which can be conveniently utilized to obtain the maximum and minimum bending deflections.

The deflections w_1 , given by equation (34) may be written as,

$$w_1 = \frac{qc^4}{Eh^3} \beta \quad (35)$$

in which, β is the dimensionless deflection coefficient.

$$\beta = \beta(x, s, \theta, N, \nu)$$

The numerical value of β provided here are for Poisson's ratio $\nu = 0.17$ (Fused Silica) and,

$$N = (3, 6, 9, 15)$$

$$s = b/c = j/10 \quad (j = 1, 2, 3, 4, 5, 6, 7, 8, 9, 10)$$

$$x = r/c = i/10 \quad (i = 1, 2, 3, 4, 5, 6, 7, 8, 9, 10)$$

$$\theta = 0, \alpha/4, \alpha/2 \quad \text{where } \alpha = 2/N$$

Since the plate is uniformly loaded and the supports are arranged in a symmetrical manner, the form of the entire deflected plate can be obtained by knowing the deflections in the shaded portion of Figure 12(a). By specifying the values of N and s , which are within the above range, the numerical values of β can be found from the tables for the

points marked with a dot (·) in Figure 12(b), corresponding to the shaded portion of Figure 12(a).

The deflection coefficient β provided here are relative to the plane of the supports. Relative to the support plane, downward deflections are positive and upward deflections are negative.

1.4 CIRCULAR PLATE ON MULTIPOINT SUPPORTS:

SUPPORTS ARE ON TWO CONCENTRIC CIRCLE

In Section 1.1, the deflection surface of a circular plate subjected to a uniform load was derived for the case when the supports of the plate were an equal distance apart from one another and on a single concentric circle. Because of the symmetrical arrangement of supports, the equations of static equilibrium are automatically satisfied, that is

1. Net force on the plate is zero.
2. Net moment of forces about the center of the plate is zero.

This section considers the case when there is more than one support circle, such that the support circles are concentric with respect to the plates and where the supports are all on the same level.

NUMERICAL METHOD

The results derived in the previous section can be utilized for some special arrangements of supports. Consider the case when a circular plate is subjected to a uniform load, and is supported as shown on Figure 13.

Since the supports on each support circle are an equal distance apart, the reactions at any point on the outer circle would be the same.

Let the reaction at any support point on the outer circle be R_2 .

Let the reaction at any support point on the inner circle be R_1 .

For equilibrium of forces

$$NR_1 + TR_2 = \pi qc^2 \quad (36)$$

For equilibrium of moments

$$b_1 R_1 \sum_{n=1}^N \cos \theta_n + b_2 R_2 \sum_{t=1}^T \cos \theta_t = 0$$

$$b_1 R_1 \sum_{n=1}^N \sin \theta_n + b_2 R_2 \sum_{t=1}^T \sin \theta_t = 0 \quad (37)$$

where,

$$\theta_n = 2\pi n/N \quad \text{and}$$

$$\theta_t = \delta + t \, 2\pi/T$$

Equation (1) can be satisfied by choosing γ such that, $0 \leq \gamma \leq 1$, and where,

$$NR_1 = \gamma \pi qc^2 \quad \text{and} \quad TR_2 = (1-\gamma) \pi qc^2 \quad (38)$$

Equations (2) are satisfied from the relations

$$\sum_{m=1}^M \sin(x+my) = \sin\left(x + \frac{M+1}{2}y\right) \sin \frac{My}{2} \operatorname{cosec} \frac{y}{2}$$

$$\sum_{m=1}^M \cos(x+my) = \cos\left(x + \frac{M+1}{2}y\right) \sin \frac{My}{2} \operatorname{cosec} \frac{y}{2}$$

When $M \neq 1$ and $y = 2\pi/M$, the above equations vanish.

The equation governing the deflection surface w for the system shown in Figure 13 is

$$\nabla^4 w = \frac{q}{D} \quad (39)$$

where,

q is the load intensity, and

D is the flexural rigidity.

A suitable solution to (39) that would satisfy equation (36) would be to take the solution to (39) as a sum

$$w = \bar{w} + w^* + A \quad (40)$$

and such that with the assumption of (38),

$$\nabla^4 \bar{w} = \frac{\gamma q}{D} \quad (41)$$

$$\nabla^4 w^* = \frac{(1-\gamma)q}{D} \quad (42)$$

Where A is a constant, which is introduced so that the deflection w can be given with reference to some datum plane.

The equations (41) and (42) can be solved in exactly the same manner as in the previous section with the boundary conditions of a free edge, so the combined system shown in Figure 13 will have the required boundary conditions of a free edge. As the method of solution of equations (41) and (42) has already been given, the deflection \bar{w} and w^* can be obtained by making the following changes in the notation of equation (34) of the previous section.

For \bar{w}

$$s \rightarrow s_1 = b_1/c \quad \text{and} \quad q \rightarrow \gamma q$$

For w^*

$$s \rightarrow s_2 = b_2/c; \quad q \rightarrow (1-\gamma)q; \quad N \rightarrow T; \quad \theta \rightarrow (\theta-\delta)$$

After making the above changes, the deflection w of equation (40) is completely defined except for the constant A. The deflection at any point on the plate can now be given with reference to the datum plane as

$$w(x, s_1, s_2, \theta, N, T, \nu) = \frac{\gamma \cdot q \cdot c^4}{Eh^3} \beta_1 + (1-\gamma) \frac{q \cdot c^4}{Eh^3} \beta_2 + A \quad (43)$$

where

$$\beta_1 = \beta(x, s=s_1, N, \theta, \nu)$$

$$\beta_2 = \beta(x, s=s_2, N=T, (\theta-\delta), \nu)$$

The deflection coefficients β_1 and β_2 can therefore be determined from the previous section, where their numerical values are provided for Poisson's ratio $\nu = 0.17$ and for various values of N and S . The following numerical example will illustrate the method of using the tables of the previous section in determining the constant γ .

EXAMPLE: To determine the deflection surface of a circular plate of radius "c", subjected to a uniform load "q" over the entire plate.

The plate is supported on three points, equal distance apart on a concentric circle of radius $b_1 (=0.5c)$, and also supported on six points, equal distance apart on a concentric circle of radius $b_2 (=0.8c)$. The offset angle δ for this problem is $\pi/6 \equiv 30^\circ$. Assume the Poisson's ratio of the plate material to be 0.17.

By equation (43), the deflection at any point of the plate for this example,

$$w(x, \theta, 0.5, 0.8, 3, 6, 0.17) = \frac{\gamma qc^4}{Eh^3} \beta_1(x, \theta, N=3, S=0.5, \nu=0.17) + (1-\gamma) \frac{qc^4}{Eh^3} \beta_2(x, \theta-\delta, N=6, S=0.8, \nu=0.17) + A \quad (44)$$

Consider the Deflection at One of the Support Points on the Inner Support Circle.

At this point $x = r/c = 0.5$, and since there is a support at $\theta = 0$, we may consider the support at $(x = 0.5, \theta = 0)$.

From the tables

$$\beta_1(x=0.5, \theta=0, S=0.5, N=3, \nu=0.17) = 0$$

$$\beta_2(x=0.5, \theta-\delta=-\delta=-30^\circ, S=0.8, N=6, \nu=0.17) = 0.137683$$

Note:

$$\beta_2(\theta - \delta) = \beta_2(\delta - \theta)$$

i.e., $\beta_2(\theta - \delta)$ in an even function.

Substituting the above values of β_1 and β_2 in equation (44), the deflection at any one of the support points on the inner support circle, with reference to the datum plane is,

$$[w]_{\text{SUPPORT}} = (1-\gamma) \frac{qc^4}{Eh^3} 0.137683 + A \quad (45)$$

Consider the Deflection at One of the Support Points on the Outer Support Circle.

At this point $x = r/c = 0.8$, and since there is a support at $\theta = \delta = 30^\circ$, we may consider the support at $(x = 0.8, \theta - \delta = 0)$.

From the tables

$$\beta_1(x=0.8, \theta=30^\circ, S=0.5, N=3, \nu=0.17) = 0.226135$$

$$\beta_2(x=0.8, \theta-\delta=0, S=0.8, N=6, \nu=0.17) = 0$$

Substituting the above values of β_1 and β_2 in equation (44), the deflection at any one of the support points on the outer support circle with reference to the datum plane is

$$[w]_{\text{SUPPORT}} = \frac{qc^4}{Eh^3} 0.226135 + A \quad (46)$$

Since all supports are in the same level, the deflection at the support points must be the same with reference to any datum plane.

Hence,

$$\text{Equation (45)} = \text{Equation (46)}$$

i.e:

$$0.137683(1-\gamma) = 0.226135\gamma$$

therefore,

$$\gamma = 0.378439$$

Hence, by equation (3)

$$R_1 = 0.126146\pi qc^2, R_2 = 0.103593\pi qc^2$$

Substituting the above value of γ in equation (45) or (46) gives the deflection at the support points with reference to the datum plane.

$$[w]_{\text{SUPPORT}} = 0.085578 \frac{qc^4}{Eh^3} + A$$

By taking $A = -0.085578 \frac{qc^4}{Eh^3}$, (i.e: Taking the datum plane as the plane of supports), the deflection at any point of the plate can be given with reference to the support points. Substituting the above values of γ and A in equation (44), the deflection, w , at any point of the plate relative to the support plane is,

$$w = \frac{qc^4}{Eh^3} (0.378439\beta_1 + 0.621561\beta_2 - 0.085578) \quad (47)$$

where,

$$\beta_1 = \beta_1(x, S=0.5, \theta, N=3, \nu=0.17)$$

$$\beta_2 = \beta_2(x, S=0.8, (\theta-30^\circ), N=6, \nu=0.17)$$

The example chosen is such that it is necessary to do the deflection analysis only for the shaded portion of the plate, shown in Figure 13; the deflection at any other point can be determined from the symmetry of the problem. With equation (47) and the numerical value provided for β 's in the previous section, the deflection, w , can be calculated. One form of graphical representation of the deflection surface, w , with respect to the radius r , ($=xc$) of the plate is shown in Figure 14. From Figure 14, the contour map of the deflected plate can be obtained. To obtain the absolute value of the deflections, the coefficients of Figure 15 have to be multiplied by the factor $(c^4 q/Eh^3)$, where q , the load intensity on the plate, c , the radius of the plate, E , modulus of elasticity and h , the thickness of the plate.

2. ANNULAR PLATE ON MULTIPOINT SUPPORTS

STATEMENT OF PROBLEM

The problem to be investigated consists of determining the deflection surface of a constant thickness annular plate of outer radius, c , and inner radius, a , subjected to the following three conditions:

1. The total load, W , is uniformly distributed with respect to the center of the plate.
2. The plate is supported by $N(N>2)$ concentrated forces, each of magnitude (W/N) , and located equal distances apart on a single concentric circle of radius b .
3. The plate has the boundary conditions of a free edge at both the inner and outer edges.

The annular plate with the above specified conditions, illustrated in Figure 16, will be referred to as System 1. The loading and support conditions on the plate of System 1 are such that the equilibrium of forces and moments are satisfied.

METHOD AND SOLUTION

The solution to the above problem will now be found on the basis of classical small-deflection theory. According to this theory, the transverse deflections, w_1 , of System 1 are characterized by

$$\nabla^4 w_1 = \frac{q}{D} \quad (48)$$

where D is the flexural rigidity and q is the uniform load intensity which is related to the total load, W , by

$$W = q\pi(c^2 - a^2) \quad (49)$$

In view of the conditions on System 1, it will be assumed that the deflections are of the form

$$w_1 = w_2 + w_3 + w_4 \quad (50)$$

such that, w_2 , w_3 and w_4 correspond respectively to the following three systems. The boundary, loading and the support conditions of these three systems are illustrated in relation to System 1 in Figure 17.

System 2. This system is a uniformly loaded annular plate of outer radius c and inner radius a . At the outer periphery the plate has the simply supported edge condition, and at the inner periphery the plate has the free edge condition. The deflection, w_2 , associated with System 2 can be obtained by the method suggested in Chapter 3 of Reference (14). Thus,

$$w_2 = \bar{K} \left\{ \left[\frac{(1-x^2)}{8} \right] \left[\frac{5+\nu}{1+\nu} - x^2 - \frac{4p^2\lambda}{\lambda+1} + \frac{8p^4}{(1-p^2)} \log p \right] \right. \\ \left. + \log x \left[\frac{\lambda p^2}{2} - p^2 x^2 + \frac{p^4(\lambda+1)}{(1-p^2)} \log p \right] \right\} \quad (51)$$

where,

$$\left. \begin{aligned} x &= \frac{r}{c} \quad , \quad p = \frac{a}{c} \\ \bar{K} &= \frac{qc^4}{8D} \quad \text{and} \quad \lambda = \frac{3+\nu}{\nu-1} \end{aligned} \right\} \quad (52)$$

The bending moment, M_{r2} , and Kirchhoff's shear, V_2 , associated with deflection, w_2 , can be found from the following expressions.

$$\left. \begin{aligned} M_{r2} &= -D \left[\nabla^2 w_2 + \frac{(1-\nu)}{c^2} \frac{\partial^2 w_2}{\partial x^2} \right] \\ V_2 &= -D \left[\frac{1}{c} \frac{\partial \nabla^2 w_2}{\partial x} + \frac{(1-\nu)}{c^3 x} \frac{\partial^2}{\partial x \partial \theta} \left\{ \frac{1}{x} \frac{\partial w_2}{\partial \theta} \right\} \right] \end{aligned} \right\} \quad (53)$$

where,

$$\nabla^2 = \frac{1}{c^2} \left[\frac{\partial^2}{\partial x^2} + \frac{1}{x} \frac{\partial}{\partial x} + \frac{1}{x^2} \frac{\partial^2}{\partial \theta^2} \right] \quad (54)$$

Thus,

$$\left. \begin{aligned} (M_{r2})_{r=c} &= 0 ; (M_{r2})_{r=a} = 0 \\ (V_2)_{r=c} &= \frac{4\bar{K}D}{c^3} (p^2-1) ; (V_2)_{r=a} = 0 \end{aligned} \right\} \quad (55)$$

System 3. The effects of concentrated supports on the plate of System 1 are accounted for by defining System 3 as a clamped circular plate of radius c , subjected to a loading condition which is identical to the support condition of System 1. The expression for the deflection, w_3 , can be obtained from the work of Michell (4). In Appendix A, the method of adapting the Michell's solution to circular plate on multipoint support is given when the total load on circular plate of System 1 is $W = q\pi c^2$. In the case when the plate of System 1 is an annular plate with outer radius c and inner radius a , and it is subjected to uniform load intensity, q , throughout, the total load is $q\pi(c^2 - a^2)$. Thus, System 3 deflection associated with an annular plate can be readily obtained by replacing W by $q\pi(c^2 - a^2)$ in equation (A6).

That is,

$$w_3 = \frac{\bar{K}}{2} \left[(x^2-1) (1-s^2) (1-p^2) + \frac{(1-p^2)}{N} \sum_{n=1}^N [x^2+s^2-2xs \cos (\theta-n\alpha)] \log \left[\frac{1+x^2s^2-2xs \cos(\theta-n\alpha)}{x^2+s^2-2xs \cos (\theta-n\alpha)} \right] \right] \quad (56)$$

where,

$$x = r/c, \quad s = b/c, \quad p = a/c$$

$$\alpha = 2\pi/N, \quad \text{and } \bar{K} = \frac{qc^4}{8D}$$

The expression for the outer edge radial bending moment, $(M_{r3})_{r=c}$, and the outer edge reaction $(V_3)_{r=c}$, associated with an annular plate, can be obtained by replacing W by $q\pi(c^2-a^2)$ in equations (A7) and (A8). That is,

$$\begin{aligned} (M_{r3})_{r=c} &= -D \left[v \nabla^2 w_3 + \frac{(1-v)}{c^2} \frac{\partial^2 w_3}{\partial x^2} \right]_{x=1} \\ &= \frac{qc^2(1-p^2)}{4N} \sum_{n=1}^N \frac{(1-s^2)^2}{[1+s^2-2s \cos (\theta-n\alpha)]} \\ &= \frac{qc^2(1-p^2)(1-s^2)}{4} \left[1 + \frac{2}{N} \sum_{n=1}^N \sum_{m=2}^{\infty} s^m \cos m(\theta-n\alpha) \right] \quad (57) \end{aligned}$$

$$\begin{aligned} (V_3)_{r=c} &= -D \left[\frac{1}{c} \frac{\partial \nabla^2 w_3}{\partial x} + \frac{(1-v)}{c^3 x} \frac{\partial^2}{\partial x \partial \theta} \left[\frac{1}{x} \frac{\partial w_3}{\partial \theta} \right] \right]_{x=1} \\ &= \frac{qc(1-p^2)}{4N} \sum_{n=1}^N \frac{(1-s^2)^3}{[1+s^2-2s \cos (\theta-n\alpha)]^2} \end{aligned}$$

$$\begin{aligned}
& + \frac{qc(1-p^2)}{4N} \sum_{n=1}^N \frac{(1-s^2)^2}{[1+s^2-2s \cos(\theta-n\alpha)]} \\
& = \frac{qc(1-p^2)}{2} \left[1 + \frac{1}{N} \sum_{n=1}^N \sum_{m=2}^{\infty} [2 + m(1-s^2)] s^m \cos m(\theta-n\alpha) \right] \quad (58)
\end{aligned}$$

The deflection, w_3 , given above will now be expanded as a trigonometric series for the region $r < b$, (i.e., $x < s$). From equation (B5) of Appendix B,

$$\begin{aligned}
& \sum_{n=1}^N (xs \cos(\theta-n\alpha)) \log [1 + x^2s^2 - 2xs \cos(\theta-n\alpha)] \\
& = -Nx^2s^2 - \sum_{n=1}^N \sum_{m=2}^{\infty} \left[\frac{1}{m-1} + \frac{x^2s^2}{m+1} \right] x^m s^m \cos m(\theta-n\alpha)
\end{aligned}$$

Therefore, from the above equation, also using equation (B1)

$$\begin{aligned}
& \sum_{n=1}^N [x^2 + s^2 - 2xs \cos(\theta-n\alpha)] \log [1 + x^2s^2 - 2xs \cos(\theta-n\alpha)] \\
& = 2Nx^2s^2 - 2N \sum_{m=N, 2N, \dots}^{\infty} (x^2 + s^2) \frac{x^m s^m}{m} \cos m\theta \\
& + 2N \sum_{m=N, 2N, \dots}^{\infty} \left[\frac{1}{m-1} + \frac{x^2s^2}{m+1} \right] x^m s^m \cos m\theta \quad (59)
\end{aligned}$$

By using the expansion formulae provided by Symonds (21), page A185, equation (6a), it can be shown for $x < s$,

$$\begin{aligned}
& \sum_{n=1}^N [x^2 + s^2 - 2xs \cos(\theta-n\alpha)] \log [x^2 + s^2 - 2xs \cos(\theta-n\alpha)] \\
& = 2N(x^2 + s^2) \log s + 2Nx^2 \\
& + 2s^2N \sum_{m=N, 2N, \dots}^{\infty} \left[\frac{1}{m(m-1)} - \frac{(x/s)^2}{m(m+1)} \right] \left(\frac{x}{s} \right)^m \cos m\theta \quad (60)
\end{aligned}$$

By using equations (59) and (60), equation (56) can be written as

$$\begin{aligned}
 w_3 = \bar{K}(1-p^2) \left\{ - \frac{(1-s^2)(1+x^2)}{2} - (x^2 + s^2) \log s \right. \\
 - \sum_{m=N, 2N, \dots}^{\infty} (x^2 + s^2) \frac{x^m s^m}{m} \cos m\theta + \sum_{m=N, 2N, \dots}^{\infty} \left[\frac{1}{m-1} + \frac{x^2 s^2}{m+1} \right] x^m s^m \cos m\theta \\
 \left. - s^2 \sum_{m=N, 2N, \dots}^{\infty} \left[\frac{1}{m(m-1)} - \frac{(x/s)^2}{m(m+1)} \right] \left(\frac{x}{s} \right)^m \cos m\theta \right\} \quad (61)
 \end{aligned}$$

Equation (61) is the expression for the deflection, w_3 , for the region $r < b$ (i.e.: $x < s$); from this expression, the bending moment, $(M_{r3})_{r=a}$ and reaction $(V_3)_{r=a}$, where $a < b$, can be found. Thus,

$$\begin{aligned}
 (M_{r3})_{r=a} = - \frac{\bar{K}D(1-p^2)}{c^2} \left\{ (1+\nu)(1-s^2+2 \log s) \right. \\
 \left. - (1-\nu) \sum_{m=N, 2N, \dots}^{\infty} \gamma_{1m} \cos m\theta \right\} \quad (62a)
 \end{aligned}$$

where,

$$\begin{aligned}
 \gamma_{1m} = \left[-s^{-(m-2)} + ms^m - (m-1)s^{m+2} \right] p^{m-2} \\
 + (m-\lambda-1) \left[s^{m+2} + \frac{s^{-m}}{m} - \frac{(m+1)s^m}{m} \right] p^m \quad (62b)
 \end{aligned}$$

and

$$(V_3)_{r=a} = \frac{\bar{K}D(1-p^2)}{c^3} \sum_{m=N, 2N, \dots}^{\infty} \gamma_{2m} \cos m\theta \quad (63a)$$

where,

$$\gamma_{2m} = \left[s^m [(1-\nu)(m^2(1-s^2) + m) - 4(1-s^2)m - 4] + s^{-m}[4 - (1-\nu)m] \right] p^{m-1}$$

$$+ (1-\nu) \left[-m^2(1-s^2) s^m - ms^{m+2} + ms^{-(m-2)} \right] p^{m-3} \quad (63b)$$

The deflection surface, w_4 , corresponding to System 4 will now be found on the reasoning that the System 1 has the boundary conditions of a free edge at $r = a$ and $r = c$. By Krichhoff's theory of plates, the boundary conditions of a free edge for the plate of System 1 are characterized by

$$(M_{r1})_{r=c} = (V_1)_{r=c} = 0 \quad (64)$$

$$(M_{r1})_{r=a} = (V_1)_{r=a} = 0 \quad (65)$$

where,

$$M_{r1} = -D \left[\nu \nabla^2 w_1 + \frac{(1-\nu)}{c^2} \frac{\partial^2 w_1}{\partial x^2} \right]$$

$$V_1 = -D \left[\frac{1}{c} \frac{\partial \nabla^2 w_1}{\partial x} + \frac{(1-\nu)}{c^3 x} \frac{\partial^2}{\partial x \partial \theta} \left\{ \frac{1}{x} \frac{\partial w_1}{\partial \theta} \right\} \right]$$

and

$$\nabla^2 = \frac{1}{c^2} \left[\frac{\partial^2}{\partial x^2} + \frac{1}{x} \frac{\partial}{\partial x} + \frac{1}{x^2} \frac{\partial^2}{\partial \theta^2} \right]$$

Substituting equation (50) in equation (64) gives

$$-(M_{r4})_{r=c} = (M_{r2})_{r=c} + (M_{r3})_{r=c}$$

and

$$-(V_4)_{r=c} = (V_2)_{r=c} + (V_3)_{r=c}$$

(66)

By using equations (55), (57) and (58), the above set of equations becomes

$$(M_{r4})_{r=c} = -\frac{2D\bar{K}}{c^3} (1-p^2)(1-s^2) \left[1 + 2 \sum_{m=N, 2N, \dots}^{\infty} s^m \cos m\theta \right] \quad (67)$$

and

$$(V_4)_{r=c} = -\frac{4KD}{c^3} (1-p^2) \sum_{m=N, 2N, \dots}^{\infty} [2 + m(1-s^2)] s^m \cos m\theta \quad (68)$$

Substituting equation (50) in equation (65) gives

$$\left. \begin{aligned} -(M_{r4})_{r=a} &= (M_{r2})_{r=a} + (M_{r3})_{r=a} \\ \text{and} \\ -(V_4)_{r=a} &= (V_2)_{r=a} + (V_3)_{r=a} \end{aligned} \right\} \quad (69)$$

By using equations (55), (62) and (63) the above set of equations becomes

$$(M_{r4})_{r=a} = \frac{KD(1-p^2)}{c^2} \left\{ (1+\nu)(1-s^2+2 \log s) - (1-\nu) \sum_{m=N, 2N, \dots}^{\infty} \gamma_{1m} \cos m\theta \right\} \quad (70)$$

and

$$(V_4)_{r=a} = \frac{\bar{K}D(1-p^2)}{c^3} \sum_{m=N, 2N, \dots}^{\infty} \gamma_{2m} \cos m\theta \quad (71)$$

where, γ_{1m} and γ_{2m} are given by equations (62b) and (63b) respectively.

The form of the boundary values for System 4, given by equations (67), (68), (70) and (71) suggests that deflections w_4 are of the form

$$\begin{aligned} w_4 &= A_0 + A_0^* \log x + B_0 x^2 \\ &+ \bar{K} \sum_{m=N, 2N, \dots}^{\infty} [A_m x^m + A_m^* x^{-m} + B_m x^{m+2} + B_m^* x^{-m+2}] \cos m\theta \end{aligned} \quad (72)$$

The boundary conditions indicate

$$\left. \begin{aligned} A_o^* &= \bar{K} p^2 [1-s^2 + (\lambda+1) \log s] \\ B_o &= \bar{K} \left[\frac{(1-s^2)}{(1+v)} - \frac{p^2}{2} (1-s^2 + 2 \log s) \right] \end{aligned} \right\} \quad (73)$$

$$\begin{aligned} A_m &= \frac{4(1-p^2)}{m\lambda(1-v)} s^m \left[(1-s^2) + \frac{(m-\lambda-1)}{m(m-1)} \right] \\ &\quad - \frac{m+1}{m-1} (m-\lambda) A_m^* - (m+1-\lambda) B_m^* \end{aligned} \quad (74)$$

$$B_m = - \frac{4(1-p^2)}{m\lambda(1-v)} s^m \left[\frac{1}{m} - \frac{s^2}{m+1} \right] + mA_m^* + (m-1)B_m^* \quad (75)$$

The constants A_m^* and B_m^* are of the form

$$A_m^* = (p^2-1)p^{2m} A_m^{**} \quad \text{and} \quad B_m^* = (p^2-1)p^{2(m-1)} B_m^{**} \quad (76a)$$

and the quantities A_m^{**} and B_m^{**} are solutions of the following pairs of simultaneous equations.

$$\left. \begin{aligned} f_m A_m^{**} + g_m B_m^{**} &= \phi_m \\ h_m A_m^{**} + k_m B_m^{**} &= \psi_m \end{aligned} \right\} \quad (76b)$$

where,

$$f_m = m(m+1)[(m-\lambda-1)p^{2(m+1)} - (m-\lambda)p^{2m} + 1]$$

$$g_m = (m-1) [(m+1)(m-\lambda-1)p^{2m} - m(m+1-\lambda)p^{2(m-1)} + m+\lambda+1]$$

$$h_m = m(m+1) [(1-\lambda-m)p^{2(m+1)} + (m-\lambda)p^{2m} + 1]$$

$$k_m = (m-1) [(m+1)(1-\lambda-m)p^{2m} + m(m+1-\lambda)p^{2(m-1)} + m+1-\lambda]$$

$$\phi_m = \frac{1}{s^m} \left[\frac{(m-\lambda-1)}{m} p^2 - s^2 \right]$$

$$\begin{aligned}
& + (m-\lambda-1)p^2 s^m \left[s^2 - \frac{(m+1)}{m} - \frac{4(1-s^2)}{(1-\nu)} - \frac{4}{m\lambda(1-\nu)} \right] \\
& + s^m \left[s^2 + m(1-s^2) + \frac{4(m-1)(1-s^2)}{\lambda(1-\nu)} + \frac{4(m-\lambda-1)}{m\lambda(1-\nu)} \right] \\
\psi_m = & \frac{1}{s^m} \left[\frac{(1-\lambda-m)}{m} p^2 + s^2 \right] \\
& - s^m \left[m(1-s^2) + s^2 + \frac{4(m-1)(1-s^2)}{\lambda(1-\nu)} + \frac{4(m-\lambda-1)}{m\lambda(1-\nu)} \right] \\
& + p^2 s^m \left[(\lambda-1)(1-s^2) + 1 + \frac{(\lambda-1)}{m} + m(1-s^2) - \frac{4(1-\lambda-m)[m(1-s^2)+1]}{m\lambda(1-\nu)} \right]
\end{aligned}$$

Substituting equations (73), (74) and (75) in equation (72) and then using equations (B1), (B4) and (B5) of Appendix B, yields the following expression for the deflection w_4 .

$$w_4 = A_0 + w_4^* \quad (77)$$

where,

$$\begin{aligned}
w_4^* = & \bar{K} \left\{ \frac{(1-s^2)}{(1-\nu)} x^2 + \frac{4(1-p^2)}{(3+\nu)} x^2 s^2 \right. \\
& + p^2 \left[(1-s^2) \left(\log x - \frac{x^2}{2} \right) + \log s \left((\lambda+1) \log x - x^2 \right) \right] \\
& - \frac{2(1-p^2)}{N(3+\nu)} \sum_{n=1}^N [x^2 + s^2 - 2xs \cos(\theta - n\alpha)] \log [1 + x^2 s^2 - 2xs \cos(\theta - n\alpha)] \\
& - \frac{8(1-p^2)}{(3+\nu)} \frac{(1+\nu)}{(1-\nu)} \sum_{m=N, 2N, \dots}^{\infty} \frac{x^m s^m}{m^2(m-1)} \cos m\theta \\
& + (p^2 - 1) \sum_{m=N, 2N, \dots}^{\infty} A_m^{**} \left[\frac{1}{x^m} - \frac{(m+1)}{(m-1)} (m-\lambda) x^m + m x^{m+2} \right] p^{2m} \cos m\theta \\
& + (p^2 - 1) \sum_{m=N, 2N, \dots}^{\infty} B_m^{**} \left[\frac{1}{x^{(m-2)}} - (m+1-\lambda) x^m + (m-1) x^{m+2} \right] p^{2(m-1)} \cos m\theta \left. \right\} \quad (78)
\end{aligned}$$

By substituting equations (51), (56) and (77) in equation (50), the constant A_0 can be evaluated by using the conditions that the deflections w_1 are zero at the support points and that w_1 is periodic with a period of $\alpha = 2\pi/N$; thus,

$$A_0 = -[w_2 + w_3 + w_4^*]_{x=s, \theta=0} \quad (79)$$

Having now formed the expressions for the deflections w_2 , w_3 and w_4 , the deflection w_1 associated with System 1 can be given in the following form

$$w_1 \frac{Eh^3}{qc^4} = \frac{3}{2} (1-\nu^2) [F_1(x,s,p) + F_2(x,s,p,\theta,N) + F_3(x,s,p,\theta,N)] \quad (80)$$

where,

$$\begin{aligned} F_1(x,s,p) = & \frac{(x^4-s^4)}{8} + p^2 s^2 \log s - p^2 x^2 \log x \\ & + p^2 \log \frac{x}{s} \left[\frac{\lambda}{2} + 1 - s^2 + \frac{p^2(\lambda+1)}{(1-p^2)} \log p + (\lambda+1) \log s \right] \\ & + (x^2-s^2) \left[\frac{\lambda}{2(\lambda+1)} - \frac{p^2}{2} \left(\frac{\lambda+2}{\lambda+1} \right) - \frac{s^2}{\lambda(\lambda+1)} + \frac{s^2 p^2}{\lambda} \right. \\ & \left. - \frac{p^4}{(1-p^2)} \log p - p^2 \log s \right] \end{aligned} \quad (81)$$

$$\begin{aligned} F_2 = & \frac{(1-p^2)}{2N\lambda} \sum_{n=1}^N (x^2 + s^2 - 2xs \cos(\theta-n\alpha)) \log \left[\frac{1+x^2 s^2 - 2xs \cos(\theta-n\alpha)}{[x^2 + s^2 - 2xs \cos(\theta-n\alpha)]^\lambda} \right] \\ & + \frac{2(1-p^2)s^2}{N\lambda} \sum_{n=1}^{N-1} \sin^2 n\alpha/2 \log \left[\frac{[2s \sin n\alpha/2]^{2\lambda}}{(1+s^4 - 2s^2 \cos n\alpha)} \right] \end{aligned}$$

$$+ \frac{(1-p^2)(\lambda^2-1)}{\lambda} \left(\sum_{m=N, 2N, \dots}^{\infty} \left[\frac{x^m s^m \cos m\theta}{m^2(m-1)} \right] - \sum_{m=N, 2N, \dots}^{\infty} \left[\frac{s^{2m}}{m^2(m-1)} \right] \right) \quad (82)$$

$$F_3 = (p^2-1) \left\{ \sum_{m=N, 2N, \dots}^{\infty} \left[A_m^{**} \frac{1}{x^m} - \frac{(m+1)}{(m-1)} (m-\lambda)x^m + mx^{m+2} \right] p^{2m} \cos m\theta \right. \\ + \sum_{m=N, 2N, \dots}^{\infty} B_m^{**} \left[\frac{1}{x^{m-2}} - (m+1-\lambda)x^m + (m-1)x^{m+2} \right] p^{2(m-1)} \cos m\theta \\ - \sum_{m=N, 2N, \dots}^{\infty} A_m^{**} \left[\frac{1}{s^m} - \frac{(m+1)}{(m-1)} (m-\lambda)s^m + ms^{m+2} \right] p^{2m} \\ \left. - \sum_{m=N, 2N, \dots}^{\infty} B_m^{**} \left[\frac{1}{s^{m-2}} - (m+1-\lambda)s^m + (m-1)s^{m+2} \right] p^{2(m-1)} \right\} \quad (83)$$

The constants A_m^{**} and B_m^{**} occurring in equation (83) are governed by equation (76).

Prior to studying the influence of size of hole, the magnitude of support circle and the number of supports on the deflection surface, some special limiting cases can be deduced from equation (80).

For the case when the plate has no hole, i.e.: $p \rightarrow 0$, the function F_3 defined by (83) vanishes and equation (80) becomes,

$$\lim_{p \rightarrow 0} \left(w_1 \frac{Eh^3}{qc^4} \right) = \frac{3}{2} (1-\nu^2) \left\{ \frac{(x^4-s^4)}{8} + \frac{(\lambda^2-2s^2)}{2\lambda(\lambda+1)} (x^2-s^2) \right. \\ + \frac{1}{2N\lambda} \sum_{n=1}^N [x^2+s^2-2xs \cos(\theta-n\alpha)] \log \left[\frac{1+x^2s^2-2xs \cos(\theta-n\alpha)}{[x^2+s^2-2xs \cos(\theta-n\alpha)]^\lambda} \right] \\ \left. + \frac{2s^2}{N\lambda} \sum_{n=1}^{N-1} \sin^2 n\alpha/2 \log \left[\frac{[2s \sin n\alpha/2]^{2\lambda}}{(1+s^4-2s^2 \cos n\alpha)} \right] \right\}$$

$$+ \frac{(\lambda^2 - 1)}{\lambda} \left\{ \sum_{m=N, 2N, \dots}^{\infty} \left[\frac{x^m s^m \cos m\theta}{m^2 (m-1)} \right] - \sum_{m=N, 2N, \dots}^{\infty} \left[\frac{s^{2m}}{m^2 (m-1)} \right] \right\} \quad (84)$$

The above equation is essentially the same as equation (34) derived in Section 1.

For the case when there are large number of supports, i.e.: $N \rightarrow \infty$ (equivalent to one continuous ring support) the function F_1 remains the same, and the function F_3 vanishes, but the function F_2 takes the form

For $x \geq s$

$$\lim_{N \rightarrow \infty} F_2 = \frac{(1-p^2)}{\lambda} [s^2(x^2-s^2) - \lambda((x^2+s^2) \log x - 2s^2 \log s)]$$

Therefore, for $N \rightarrow \infty$ and $x \geq s$, equation (80) becomes

$$\begin{aligned} \lim_{N \rightarrow \infty} \left(w_1 \frac{Eh^3}{qc^4} \right) &= \frac{3}{2} (1-\nu^2) \left\{ \frac{(x^4-s^4)}{8} + 2s^2 \log s - (x^2+s^2) \log x \right. \\ &+ p^2 \log \frac{x}{s} \left[\frac{\lambda}{2} + 1 + p^2 \frac{(\lambda+1)}{(1-p^2)} \log p + (\lambda+1) \log s \right] \\ &\left. + (x^2-s^2) \left[\frac{\lambda}{2(\lambda+1)} - \frac{p^2(\lambda+2)}{2(\lambda+1)} + \frac{s^2}{(\lambda+1)} - \frac{p^4}{(1-p^2)} \log p - p^2 \log s \right] \right\} \quad (85) \end{aligned}$$

and for $N \rightarrow \infty$, and $x \leq s$, equation (80) takes the form

$$\begin{aligned} \lim_{N \rightarrow \infty} \left(w_1 \frac{Eh^3}{qc^4} \right) &= \frac{3}{2} (1-\nu^2) \left\{ \frac{(x^4-s^4)}{8} + p^2 s^2 \log s - p^2 x^2 \log x \right. \\ &\left. + p^2 \log \frac{x}{s} \left[\frac{\lambda}{2} + 1 - s^2 + p^2 \frac{(\lambda+1)}{(1-p^2)} \log p + (\lambda+1) \log s \right] \right\} \end{aligned}$$

$$+ (x^2 - s^2) \left\{ \frac{p^2}{2} \left(\frac{\lambda}{\lambda+1} \right) - \frac{\lambda+2}{2(\lambda+1)} + \frac{s^2}{(\lambda+1)} - \frac{p^4}{(1-p^2)} \log p - \log s \right\} \quad (86)$$

The deflection surface w_1 defined by equations (85) and (86) could also be derived by the method suggested in chapter 3 of Reference (14).

RESULTS AND DISCUSSION

The expression given for deflection, w_1 , by equation (80) is rather long for numerical computation by conventional desk calculating machines. However, using relatively simple computer programs, one could extract information of practical interests from this equation. The results of using such programs are illustrated in Figures 18 to 21. In developing these figures Poisson's ratio ν is taken as 0.17, which corresponds to fused silica.

Figure 18 shows the relation between the nondimensional hole size and the optimum value for the nondimensional radius of the support circle for a uniformly loaded annular plate on multipoint supports. The optimum size for the support circle here means that the size of the support circle for which the peak-to-peak displacement is minimum. This information is of practical interest in testing of optical flats and in the preliminary design of mirrors for optical telescopes. In the case of three point supports, Emerson (25) states that the optimum position for the support circle is 0.7 of the radius of the plate. His conclusions are, however, based on measuring deflections along a single line for different support positions. In reviewing Emerson's

results and techniques, Dew (26) remarks that the overall least sag for three point support of optical flats can be achieved by supporting them at 0.6 of the flat. The present theoretical investigation, however, indicates this quantity to be 0.66.

Pearson (27) in his paper, "Effects of the Cassegrain Hole on Axial Ring Supports," investigates the optimum size for the support circle when the support is a continuous ring. The analytical expressions derived for the displacements by Pearson are the same as the equations (85) and (86), except that he uses the outer edge of the plate as a datum instead of the plane of the supports. Since the optimum size for the support circle depends only on the relative magnitudes of the peak-to-peak displacements, the choice of the datum plane does not effect the final results: the curve obtained by Pearson and the dotted curve shown in Figure 18 are the same.

It seems from literature on optical mirror design that the optical engineers would prefer a fewer number of discrete point supports rather than a continuous ring support; but henceforth, there was no analytical expression for the displacements available for an annular plate on discrete point supports. In this respect, data provided by Figure 18 would be of practical value.

It was found from the point of view of graphical representation, that when the number of supports is 12 or above, the optimum radius for the support circle is almost the same as the radius of optimum continuous ring support. For comparison purposes, Figure 19 is drawn to indicate the magnitude of peak-to-peak displacements for a given hole size and when the supports are at the optimum positions. Figures

20 and 21 are respectively the contour maps for a uniformly loaded annular plate on three equally spaced point supports; in Figure 20, the supports are not at the optimum positions, and Figure 21 gives the contour map when the supports are situated at the optimum positions.

SUMMARY

Based on classical linear theory of plates, the deflection of a symmetrically loaded circular plate supported at discrete points equally spaced along the circumference of a concentric circle are derived. It is assumed in the formulation that the plate material is isotropic and the plate is of constant thickness. Explicit expressions for the plate deflection are given for a number of types of loading. A procedure is also outlined for obtaining contour maps of uniformly loaded circular plates with discrete supports on two concentric support circles. Analytical expression for the deflection of a uniformly loaded annular plate supported at discrete points is also developed.

The above class of problems has been investigated previously by a number of authors, utilizing different methods. However, all of the available techniques have certain limitations in their applicability to practical problems.

In the case of circular plates, there are a number of papers utilizing the techniques of functions of a complex variable. The solutions available by this method, even though mathematically elegant and rigorous, require a considerable amount of complicated analysis before they can be utilized by an engineer on practical problems. Also, at

present there is no established solution for an annular plate on multipoint supports which utilizes functions of a complex variable. Because of the difficulties associated with using the complex variable technique, a number of authors have adapted Clebsch's method for solving plates on discrete supports.

Clebsch's method has merit over the complex variable method only in the sense that the analysis is conducted and the final results are obtained in terms of real variables. The notable difficulty with this method is that the analysis can be tedious and the final results often tend to be in a cumbersome form. The main reason for the latter is that his method gives the singular terms associated with the problems in terms of an infinite series, which makes the manipulation difficult if not impossible. Further, in the neighborhood of the concentrated supports, convergence of the series is rather slow.

Another well-known approach to plates on multipoint supports is due to Nadai (13). This method utilizes real analysis, but its applications are limited to the case when supports are at the periphery.

In this dissertation, a single procedure is adapted to investigate both the circular and annular plates on multipoint supports. By the selected procedure, all the analysis and the derived expressions for the deflections are in terms of real variables. Therefore, the results would be more meaningful to a broad spectrum of engineers. With the present method, the radius of the support circle can be as large as the size of the plate itself or as small as the size of the hole of the annular plate. Therefore, the derived solution contained herein for an annular plate on multipoint supports is the first of its kind.

The procedure adapted herein yields a much more compact and appealing solution to the present class of problems than the same problems approached by means of Clebsch's method. The relative compactness of the derived results enables one to consider a large class of surface loadings. Furthermore, the infinite series terms that occur in the problems considered herein are due to boundary conditions and not due to singularities associated with the problem, and therefore, the rate of convergence is better. The simplicity of the procedure adapted may find use for the investigations of various related problems that have not been considered here but could occur in practice.

In essence, the procedure adapted herein for handling plates on discrete supports utilizes only the superposition principle. Prior to using this principle, however, it was noted from the investigations of other authors that the difficulty associated with the present class of problems is due mainly to handling the singular terms arising in the problems. By realizing this fact, the singular terms are kept in the present analysis in a compact form so that numerical manipulation may be performed with ease. The singular terms associated with the problems considered here are constructed by extending Michell's inversion procedure (4).

The results are verified by comparing published experimental results of others for the case of a uniformly loaded plate with three discrete supports. A design chart is also drawn. This chart gives the theoretical optimum size of the support circle that would produce least peak-to-peak displacements for any given size of hole and a specified number of supports. To show the influence of the size of the support

circle, contour maps of deflections are drawn for a uniformly loaded annular plate on three discrete supports.

This dissertation provides a simplified approach to the solution of circular and annular plates on discrete supports. This approach leads to a solution which is compact and appealing for use by practicing engineers.

REFERENCES

- (1) S. D. Poisson, *Sur le Mouvement des Corps Elastiques*, Memoirs de l'Academie Royale des Sciences de L'Institut de France, Vol. 8, p. 545, 1829.
- (2) A. Clebsch, *Theorie der Elasticitaet Fester Koerper*, Leipzig, Germany, 1862; French edition by Barre de Saint-Venant, *Theorie de l'Elasticite des Corps Solides*, Paris, 1883.
- (3) A. Foepppl, *Die Biegung einer Kreisfoermigen Platte*, Sitzungsberichte Bayerische Academic Wiss., Vol. 42, p. 154, 1912.
- (4) J. H. Michell, *The Flexure of a Circular Plate*, Proceedings of the London Mathematical Society, Vol. 34, p. 223, 1902.
- (5) E. Malan, *Die Durchbiegung Einer Exzentrish Durch eine Einzellast Belastelen Kriesplatte*, Der Eisenbau, Vol. 11, p. 190, 1920.
- (6) S. G. Lechnitskii, *J. Appl. Math. Mech.* Vol. 2, p. 181, 1938.
- (7) A. L. Lurie, *J. Appl. Math. Mech.*, Vol. 4, p. 93, 1940.
- (8) M. M. Friedmann, *Akad, Nauk SSSR. Prikl. Mat. Mech.*, Vol. 15, p. 258, 1951.
- (9) G. G. Chankvetadze, *Ingen. Sb.* Vol. 14, p. 73, 1953.
- (10) K. Washizu, *Trans. Soc. Mech. Engrs. Japan*, Vol. 18, p. 41, 1952.
- (11) Y. Y. Yu, *J. Appl. Mech.*, Vol. 21, p. 129, 1954.
- (12) W. A. Bassali, *The Transverse Flexure of Thin Elastic Plates Supported at Several Points*, *Proc. Cambridge Phil. Soc.*, Vol. 53, p. 728, 1957.

- (13) A. Nadai, *Die Verbiegungen in einzelnen Punkten unterstützter Kreisformiger Platten*, *Physikalische Zeitschrift*, Vol. 23, p. 336, 1922.
- (14) S. Timoshenko and S. Woinowsky-Krieger, "Theory of Plates and Shells," 2nd Ed., New York, McGraw-Hill Book Co., 1959.
- (15) C. DeBeer, *Ingenieur*, 1946.
- (16) W. A. Bassali, *Thin Circular Plates Supported at Several Points Along the Boundary*, *Proc. Cambridge Phil. Soc.*, Vol. 53, p. 525, 1957.
- (17) J. C. L. Yu and H. H. Pan, *Uniformly Loaded Circular Plates Supported at Discrete Points*, *Int. J. Mech. Sci.*, Vol. 8, p. 333, 1966.
- (18) A. W. Leissa and L. T. Wells, *On a Direct Fourier Solution for Circular Plates Loaded by Singularities*, *The Journal of the Industrial Mathematics Society*, Vol. 20, part 1, p. 1, 1970.
- (19) K. Girkmann, *Flachentragwerke*, 5th Ed., Wien, Springer-Verlag, 1959.
- (20) H. Reissner, *Bending and Buckling of Elastically Restrained Circular Plate*, *Journal of Applied Mechanics*, Vol. 19, p. 167, 1952.
- (21) P. S. Symonds, *Concentrated Force Problems in Plane Strain, Plane Stress, and Transverse Bending of Plates*, *Journal of Applied Mechanics*, Vol. 68, p. A-183, 1946.
- (22) H. Reissner, *Über die Unsymmetrische Biegung dünner Kreisrinnenplatten*, *Ingenieur Archiv*, Vol. 1, p. 72, 1929.

- (23) R. Amon and D. E. Widera, *Clamped Annular Plate under a Concentrated Force*, AIAA Journal, Technical Notes, Vol. 7, p. 151, 1969.
- (24) M. E. Agabein, S. L. Lee and J. Dandurs, *Bending of an Annular Slab Supported on Columns*, Journal of the Franklin Institute, Vol. 284, p. 300, 1967.
- (25) W. B. Emerson, *Determination of Planeness and Bending of Optical Flats*, Journal of Research of the National Bureau of Standards, Vol. 49, p. 241, 1952.
- (26) G. D. Dew, *Systems of Minimum Deflection Supports for Optical Flats*, Journal of Scientific Instruments, Vol. 43, p. 809, 1966.
- (27) E. T. Pearson, *Effects of the Cassegrain Hole on Axial Ring Supports*, "A Symposium on Support and Testing of Large Astronomical Mirrors," Edited by D. L. Crawford, A. B. Meinel and Martha W. Stockton, University of Arizona, July, 1968.
- (28) I. S. Gradshteyn and I. M. Ryzhik, "Table of Integrals, Series and Products," 4th Ed., New York, Academic Press, 1965.
- (29) L. B. W. Jolley, "Summation of Series," 2nd Ed., New York, Dover Publications, Inc., 1961.

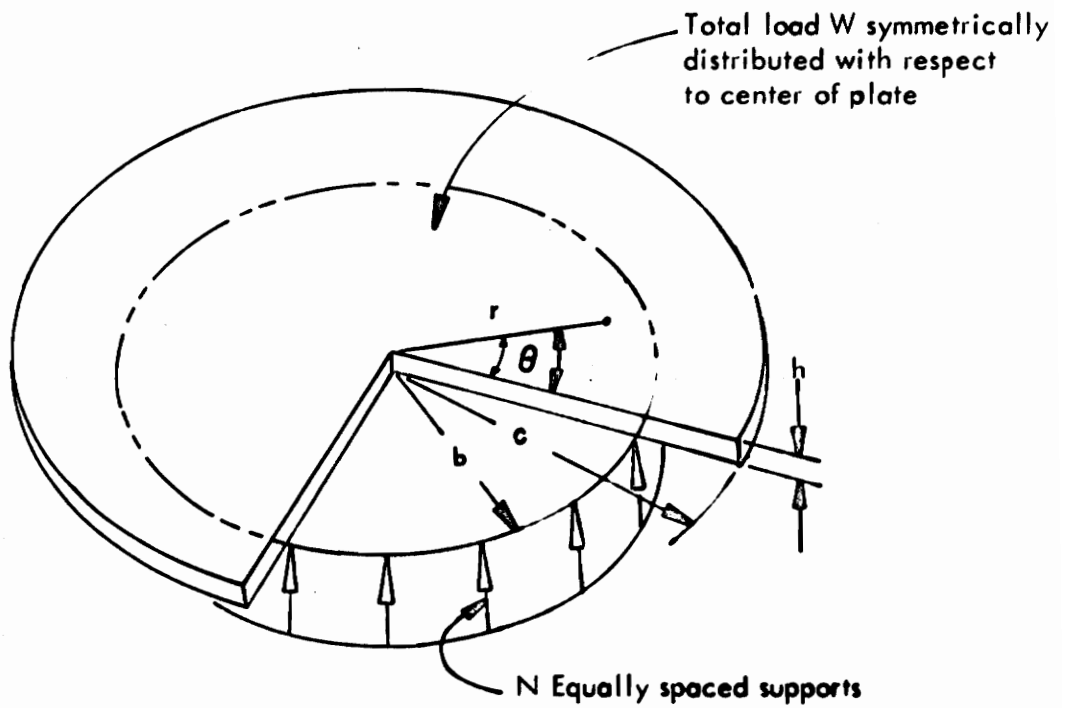


FIGURE 1. Symmetrically loaded circular plate with multipoint supports

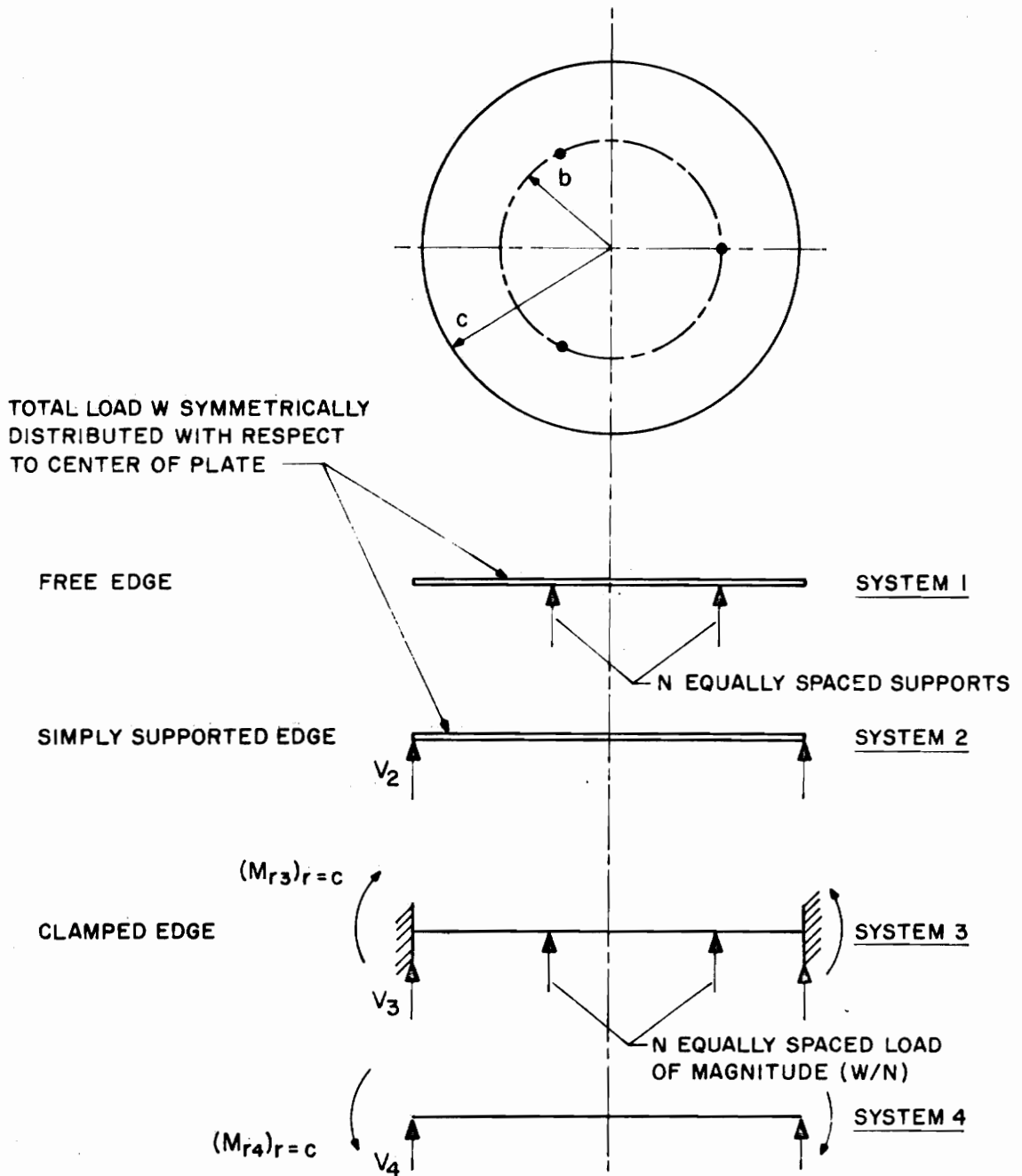


FIGURE 2. System 1 in relation to System 2, 3, and 4

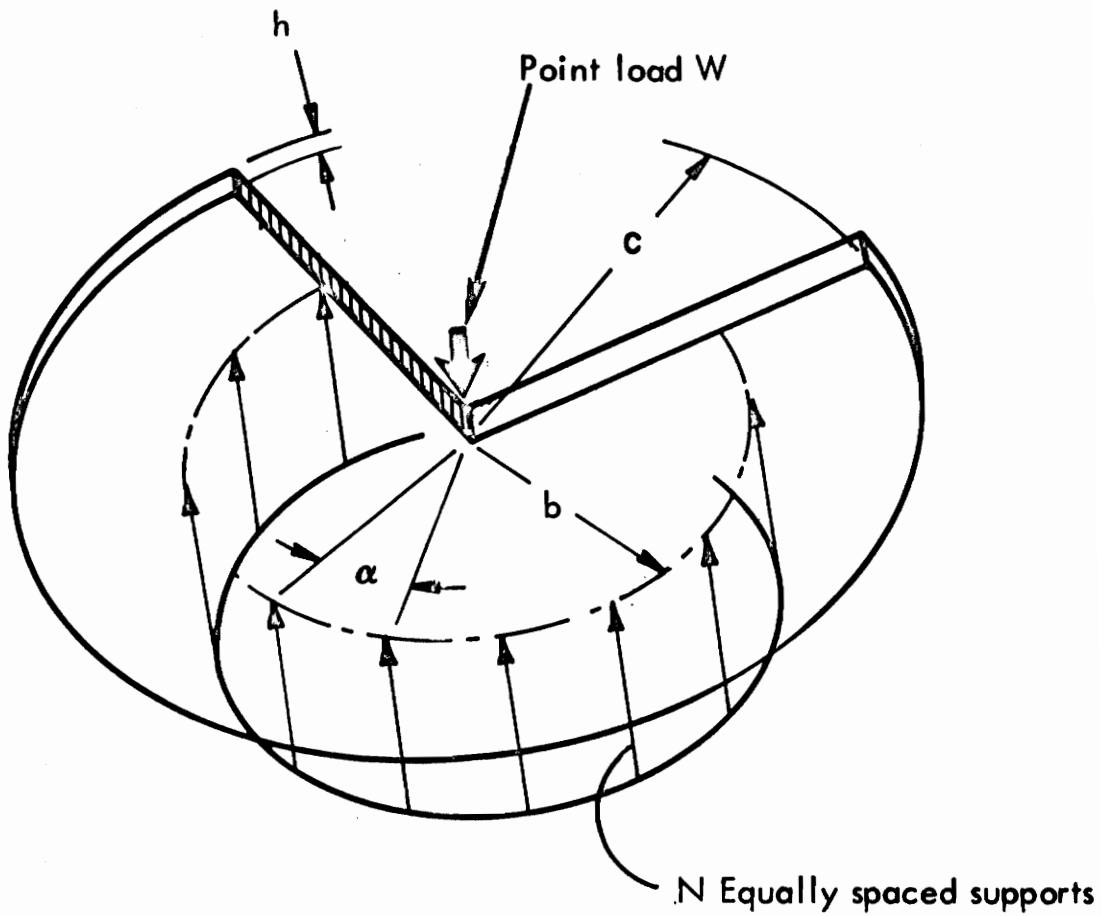


FIGURE 3. Circular plate on multipoint supports subjected to a concentrated force at center

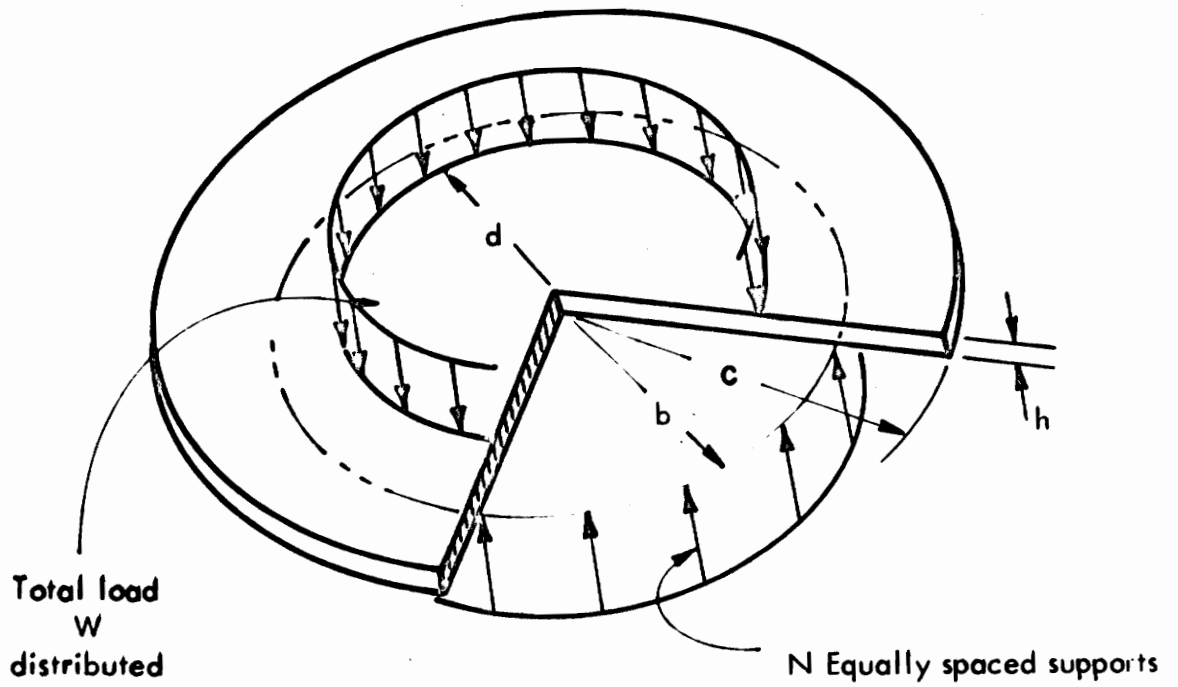


FIGURE 4 . Circular plate on multipoint supports subjected to a uniformly distributed load along a concentric ring

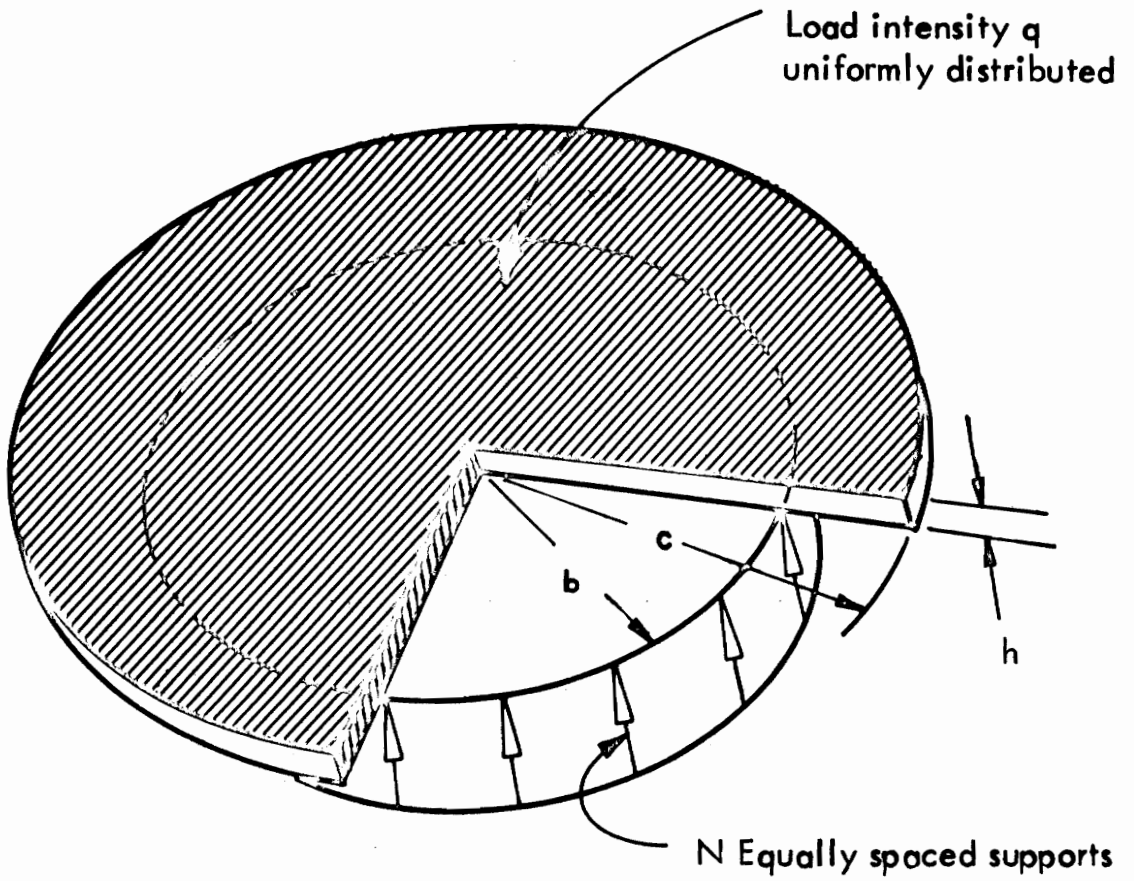
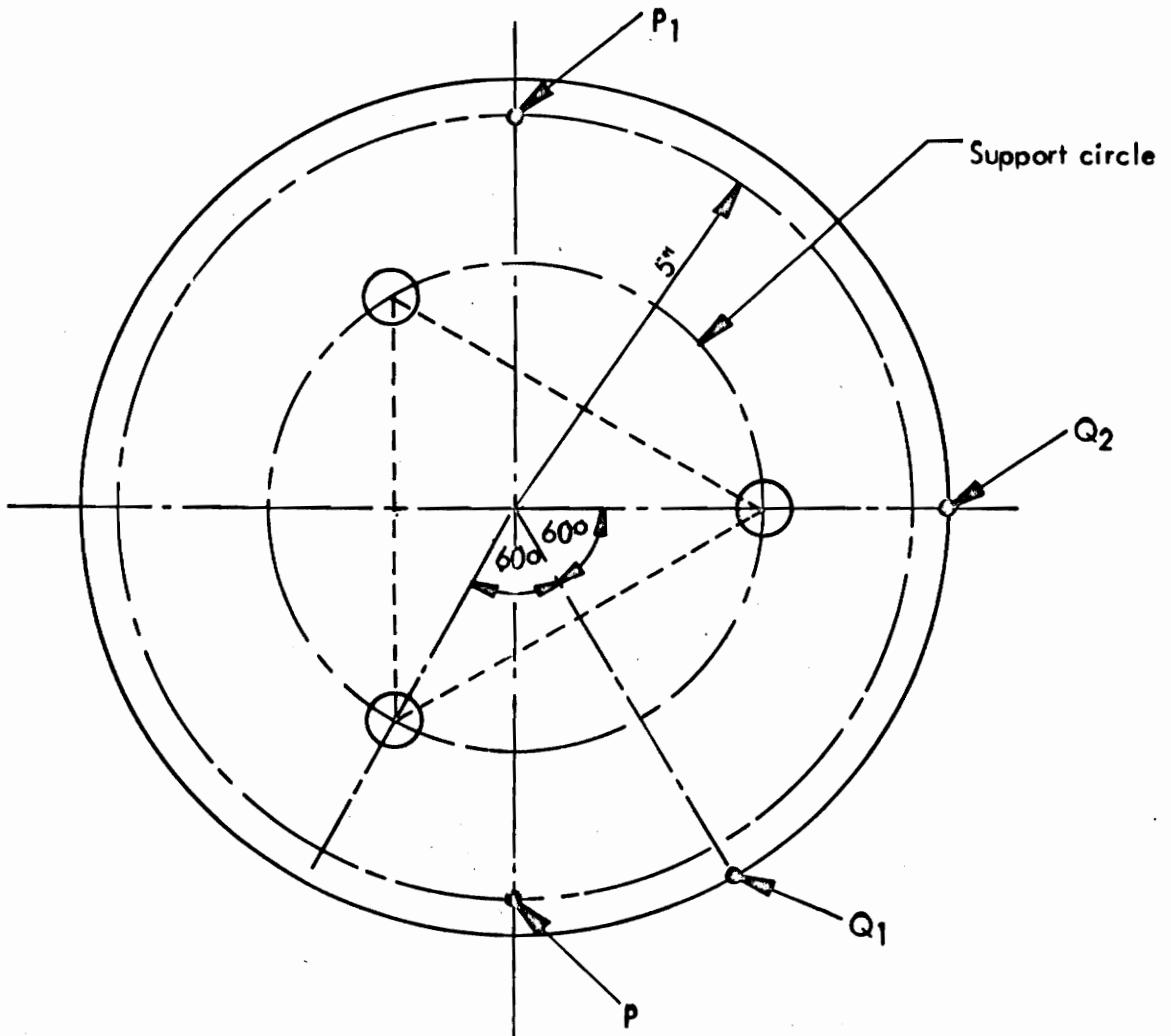


FIGURE 5. Uniformly loaded circular plate with multipoint supports



Radius of the plate,	$c = 5.33$ Inches
Thickness of specimen	$h = 1.428$ Inches
Weight of plate,	$W = 10.18$ Pounds
Modulus of elasticity	$E = 10.15 \times 10^6$ Pounds/Inch ²
Poissons ratio	$\nu = 0.14$
Number of supports	$N = 3.0$

$$0.177 \text{ Fringe} = 2.05 \times 10^{-6} \text{ Inches}$$

FIGURE 6. Details of the experimental specimen (from Reference 25)

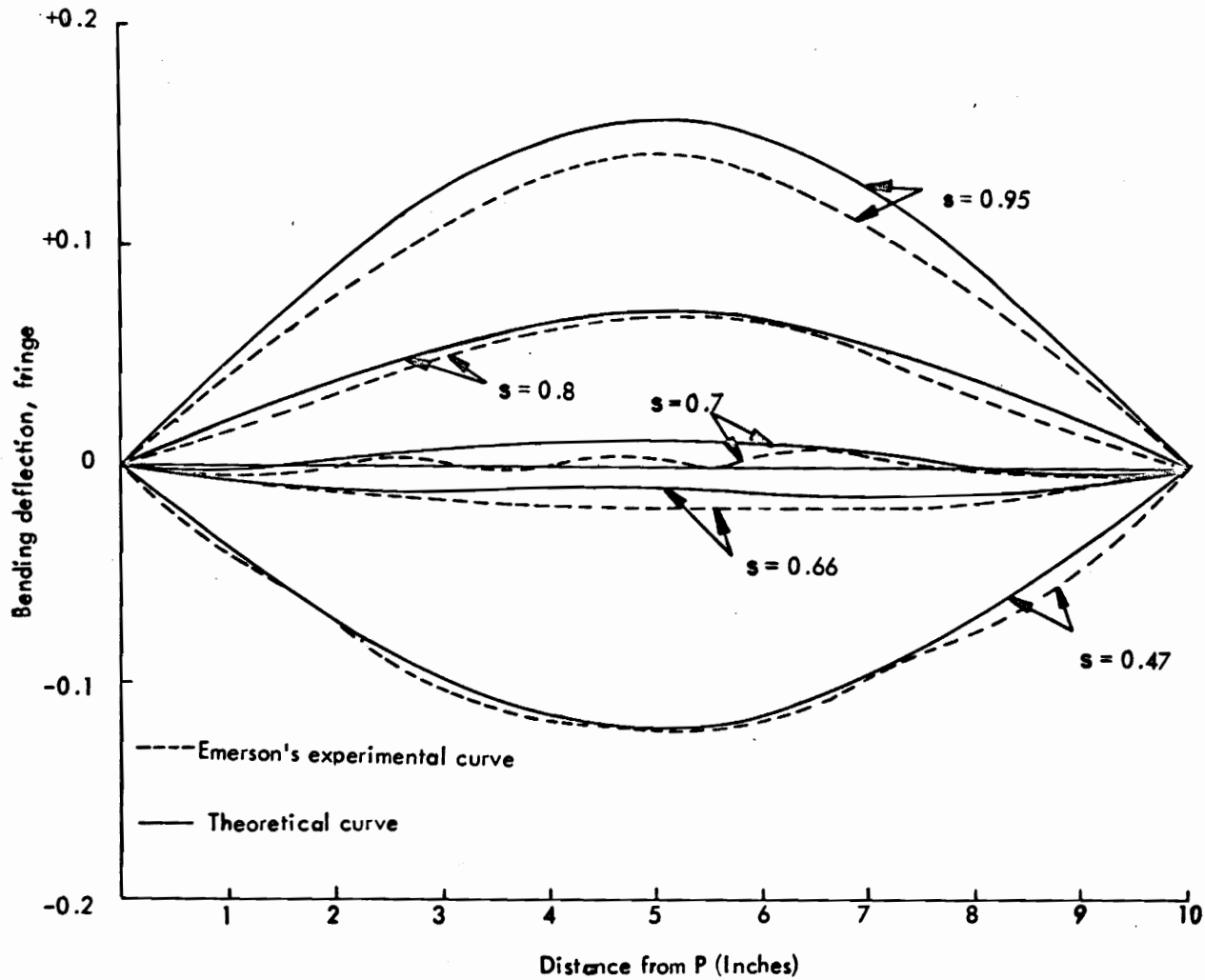


FIGURE 7. Theoretical and experimental bending curves for the plate (Figure 6) supported at different distances from its center. (Relative to the point P and P_1 , the positive values are downward deflection and the negative values are upward deflection.)

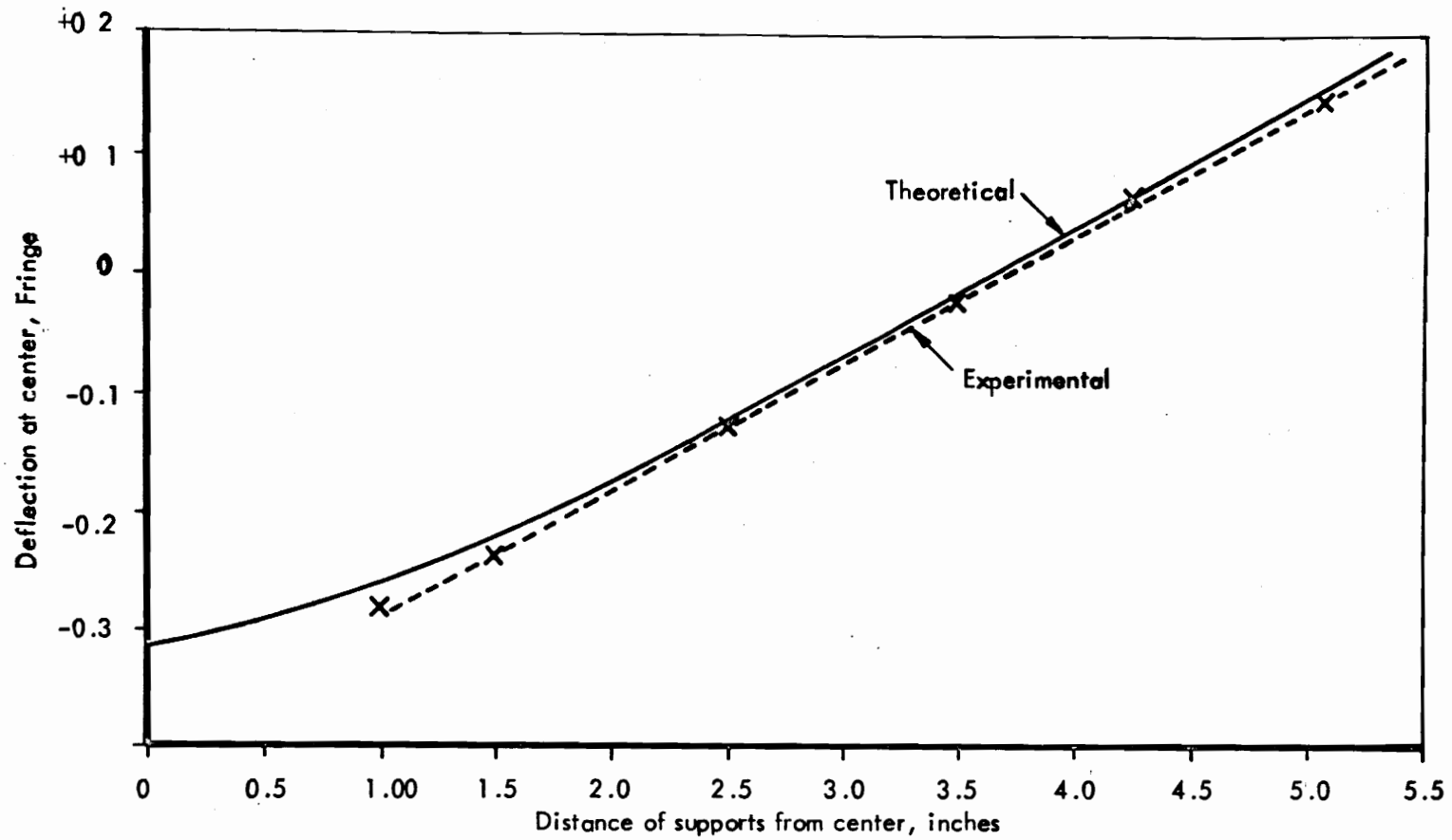


FIGURE 8. Theoretical and experimental bending deflection at the center of plate (Figure 6) Relative to points P and P₁, for supports at different distances from the center. (Relative to the point P and P₁, the positive values are downward deflection and the negative values are upward deflection.)

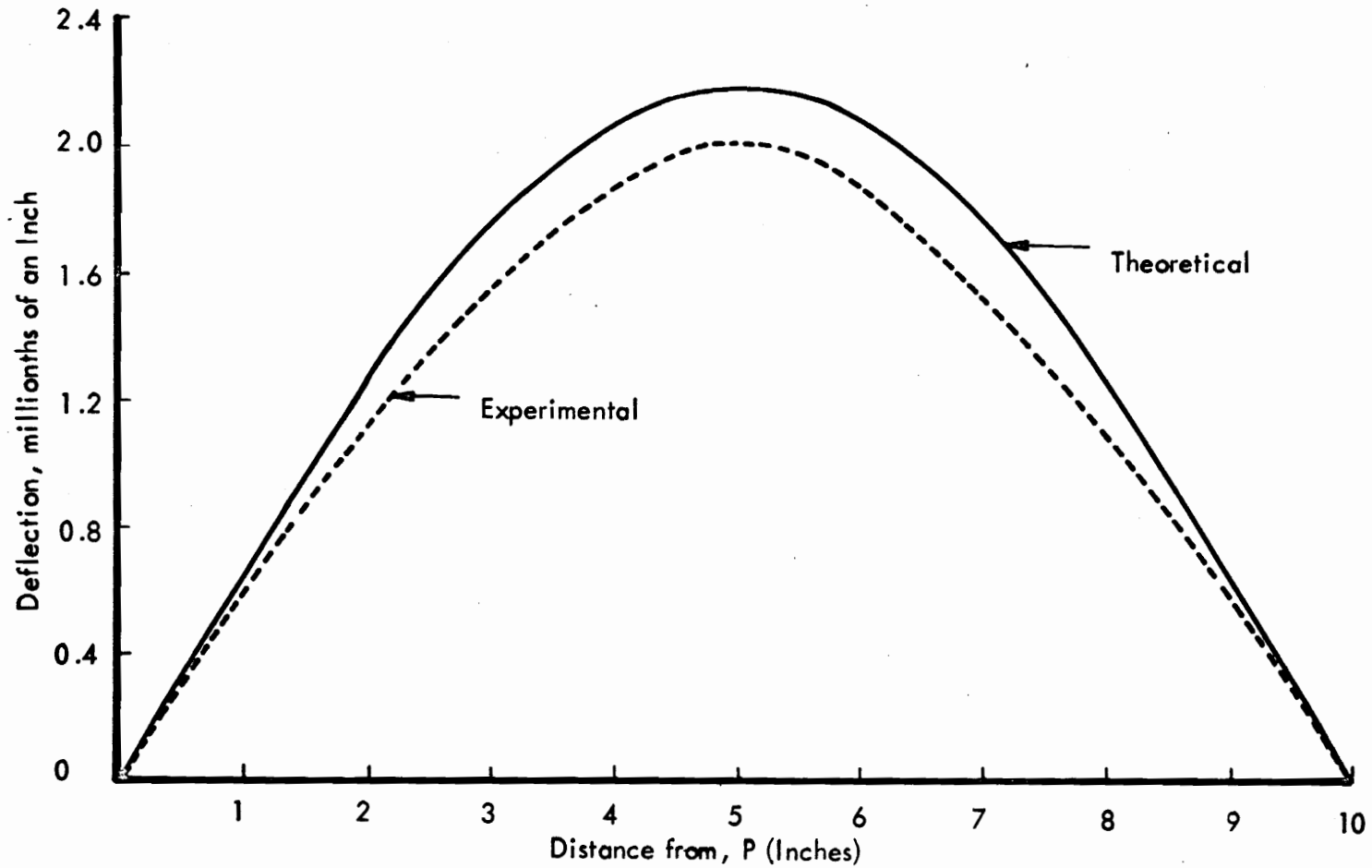


FIGURE 9. Theoretical and experimental bending curves for the plate (Figure 6) supported at three equally spaced points on its circumference. The curves give the difference in the bending deflection at points along a diametric line that is parallel to two of the supports and the deflection at points on the same line that are five inches from the center of the plate.

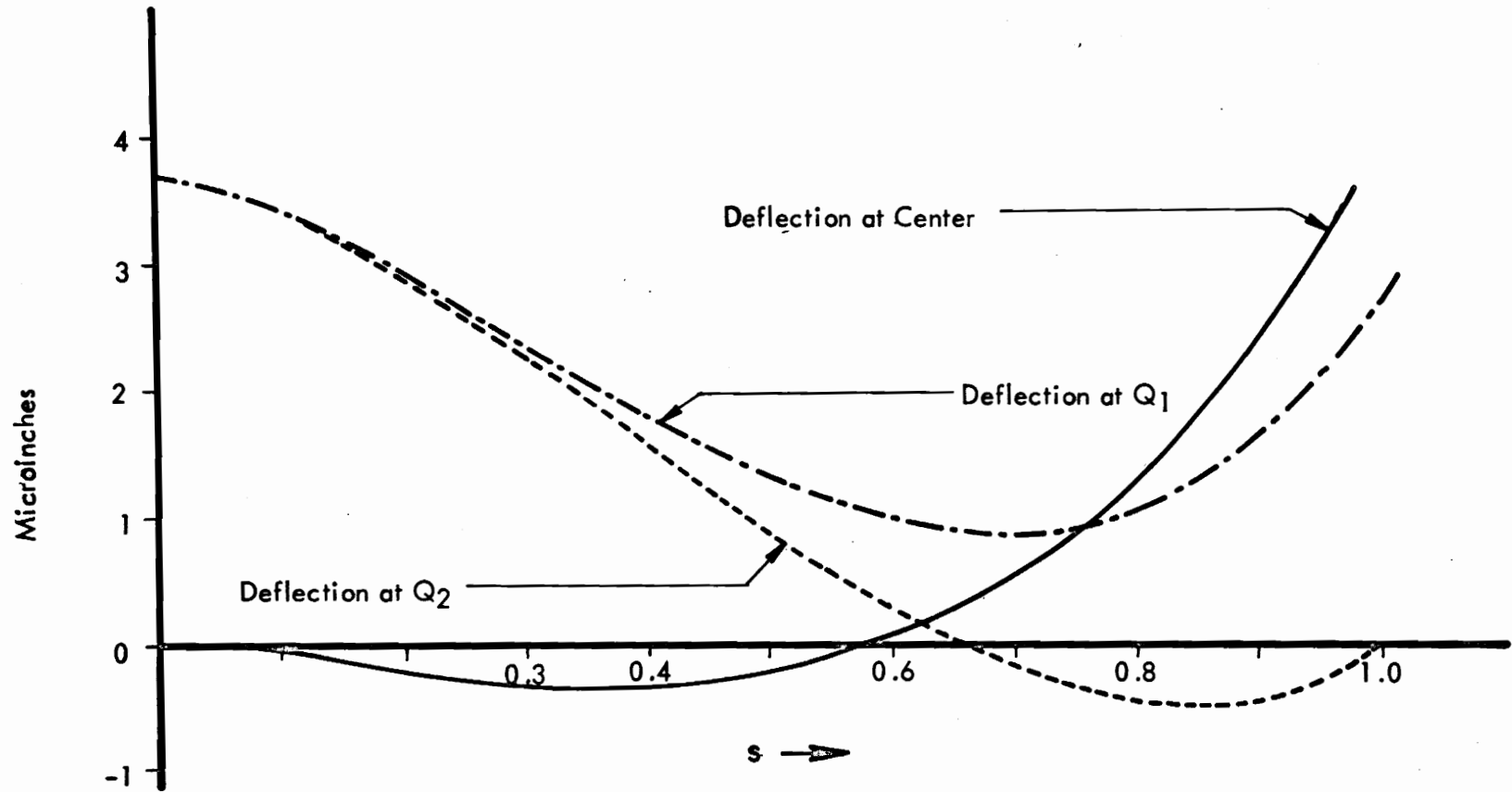


FIGURE 10. Curve showing the theoretical bending deflection at the point Q_1 , Q_2 and at the center for the plate (Figure 6), for different S values. Relative to the plane of supports, the positive values are downward deflection, and the negative values are upward deflection.

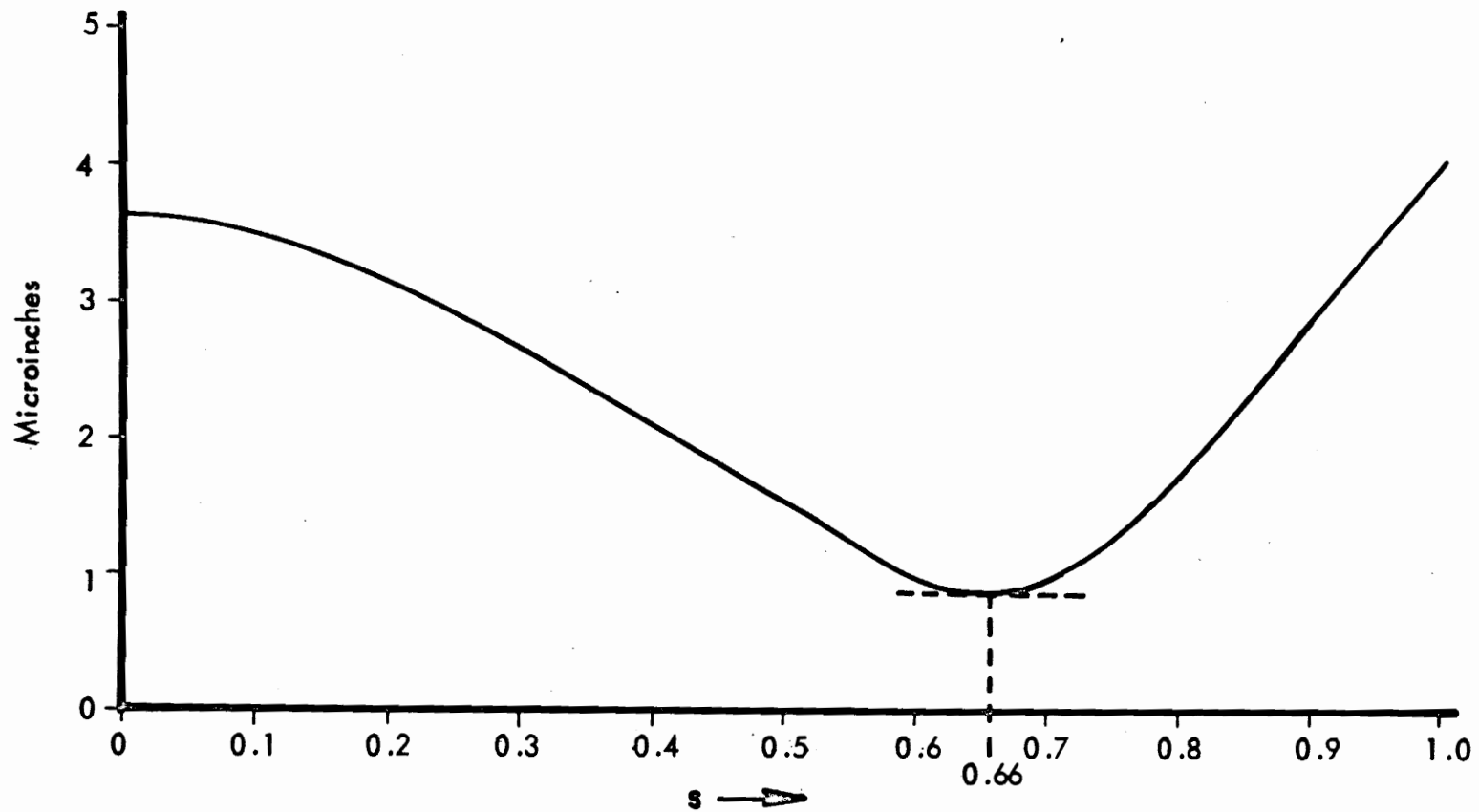


FIGURE 11. Curve showing the maximum deviation in the theoretical bending deflection of the circular plate (Figure 6) for different S values.

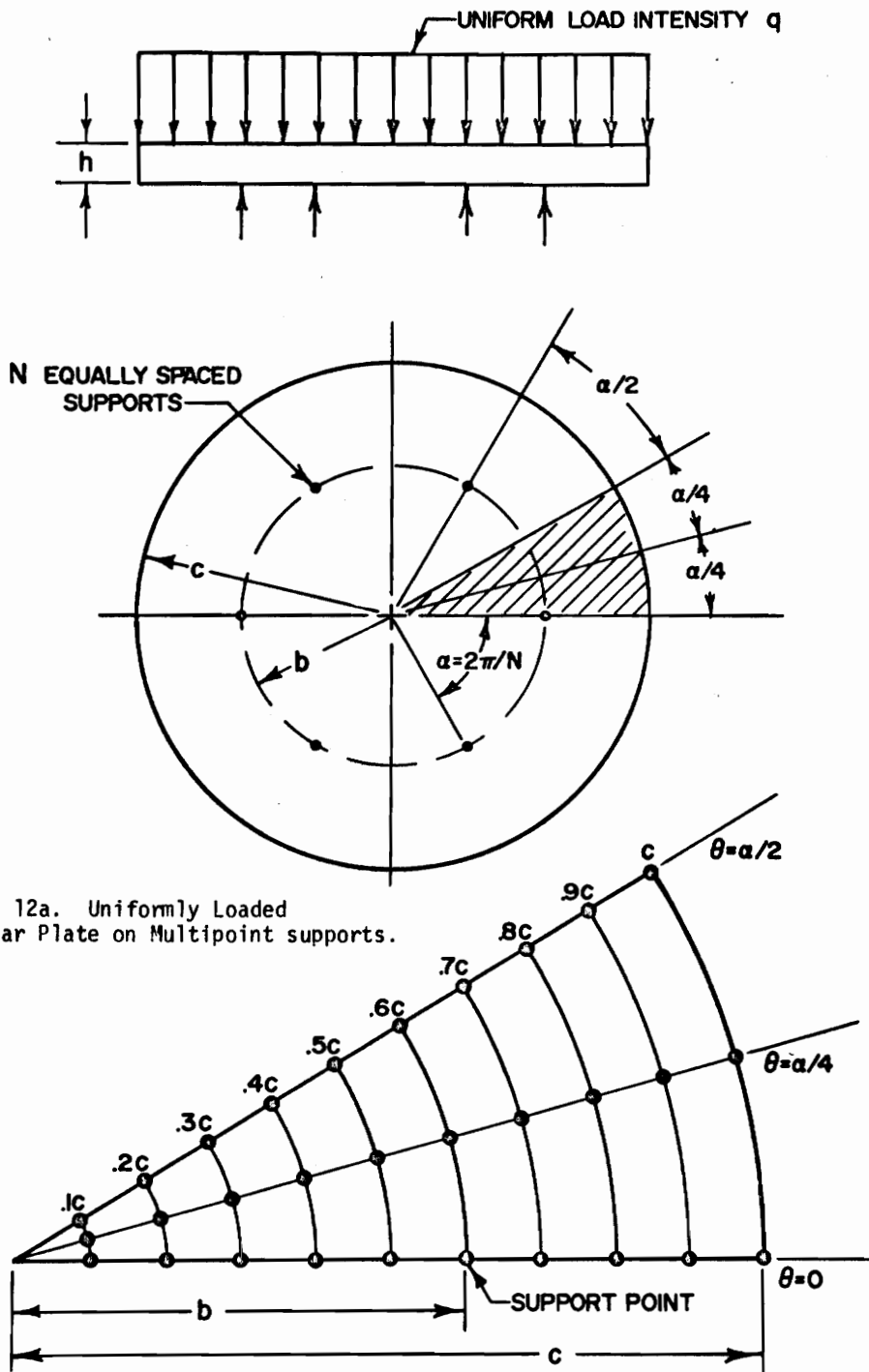


FIGURE 12a. Uniformly Loaded circular Plate on Multipoint supports.

FIGURE 12b. Shaded Portion of Figure 12a.

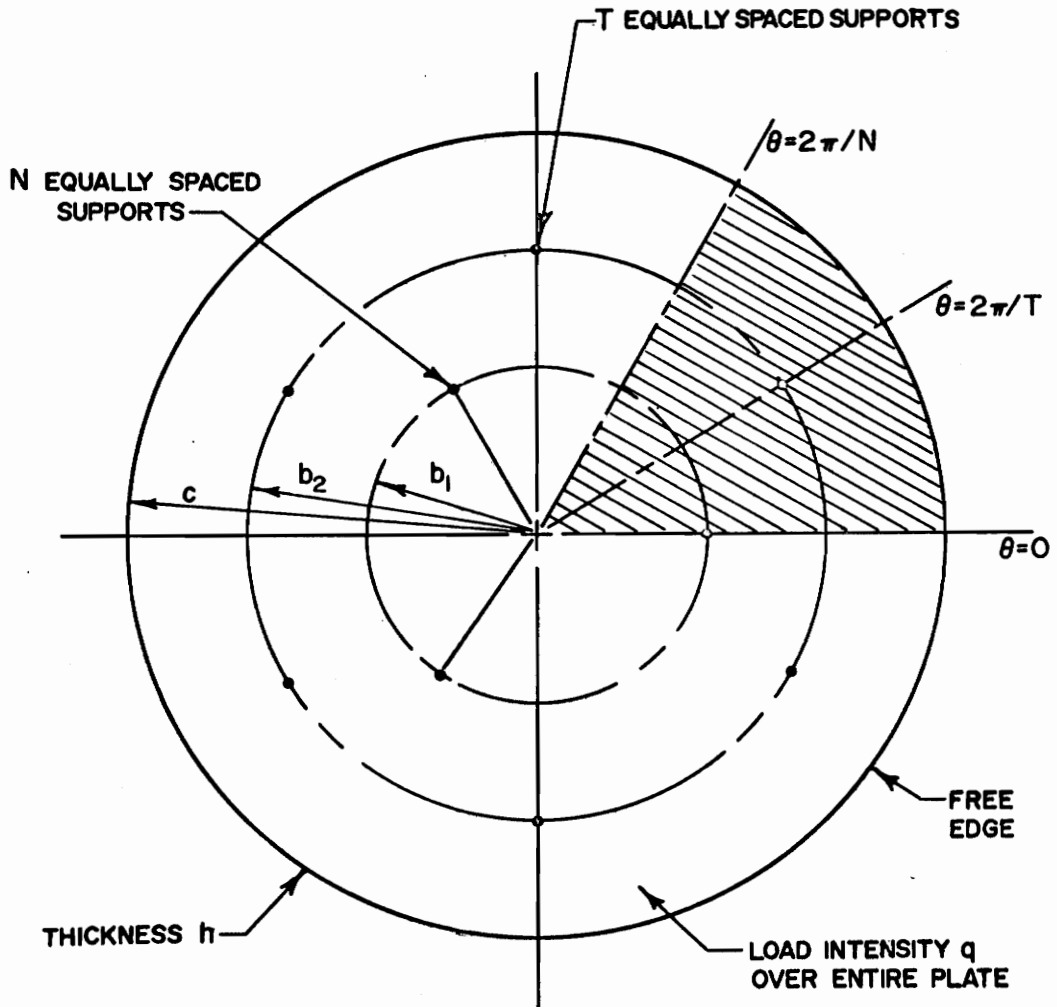


FIGURE 13. Circular Plate on Multipoint Supports; Supports are situated in two support circles.

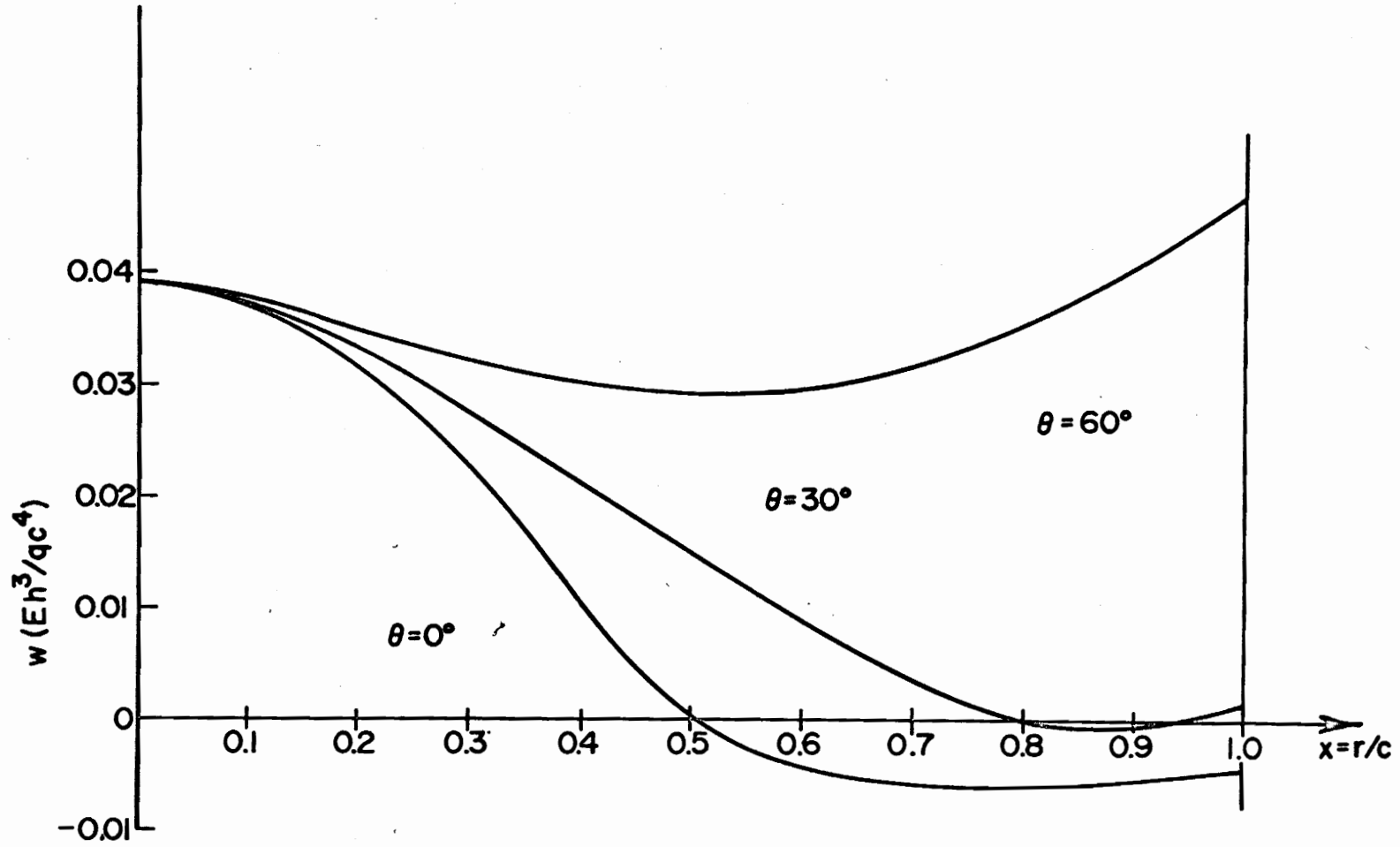


FIGURE 14. Curve representing the deflection w of the Plate, shown in Figure 13; from the center of the Plate to the edge of the Plate along the Line $\theta = 0, 30^\circ$, and $\theta = 60^\circ$.

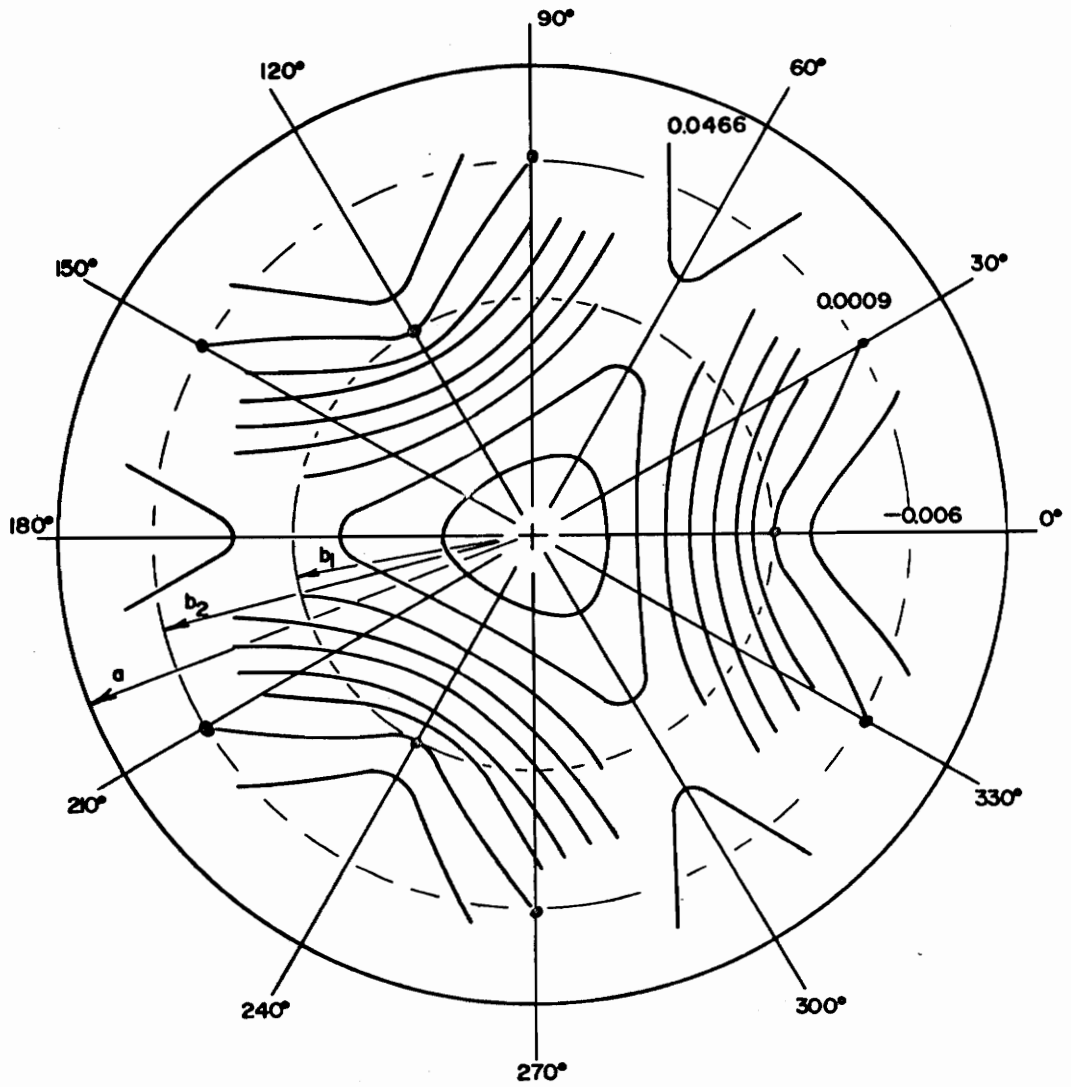


FIGURE 15. Contour map of Plate shown in Figure 13.

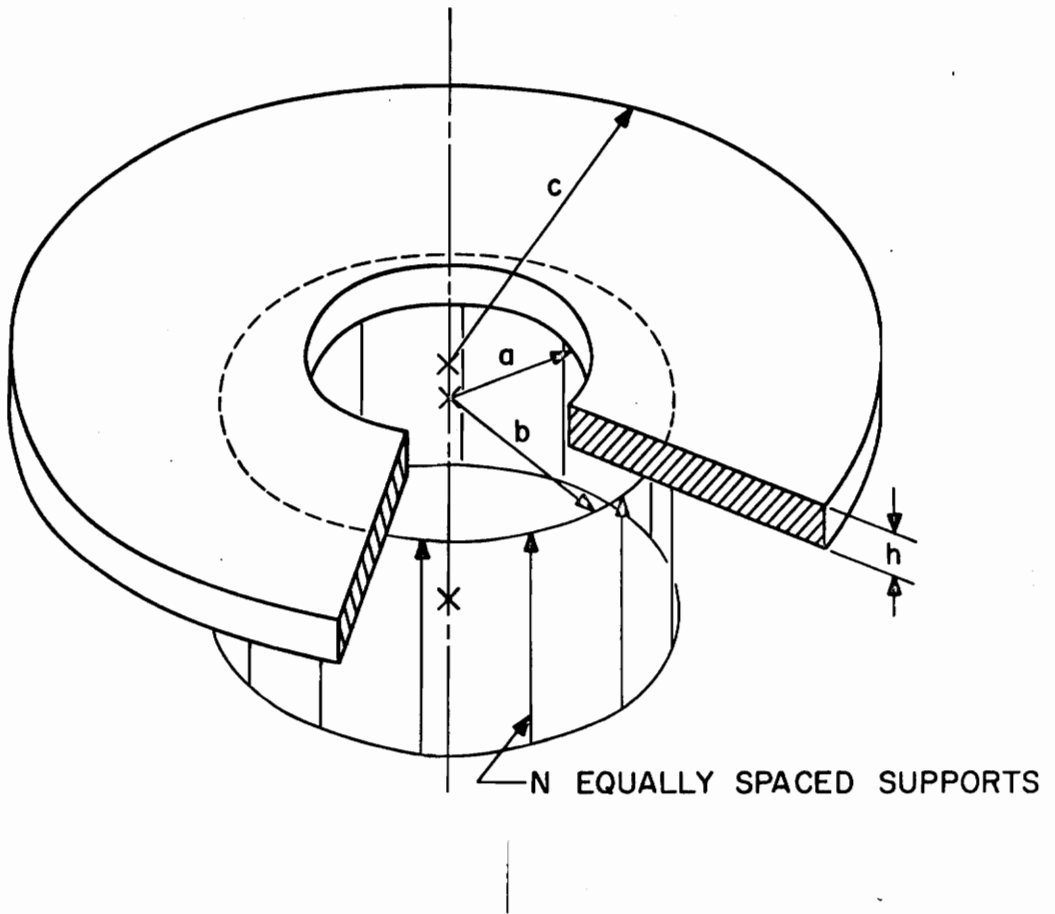


FIG. 16. UNIFORMLY LOADED ANNULAR PLATE ON MULTIPOINT SUPPORTS.

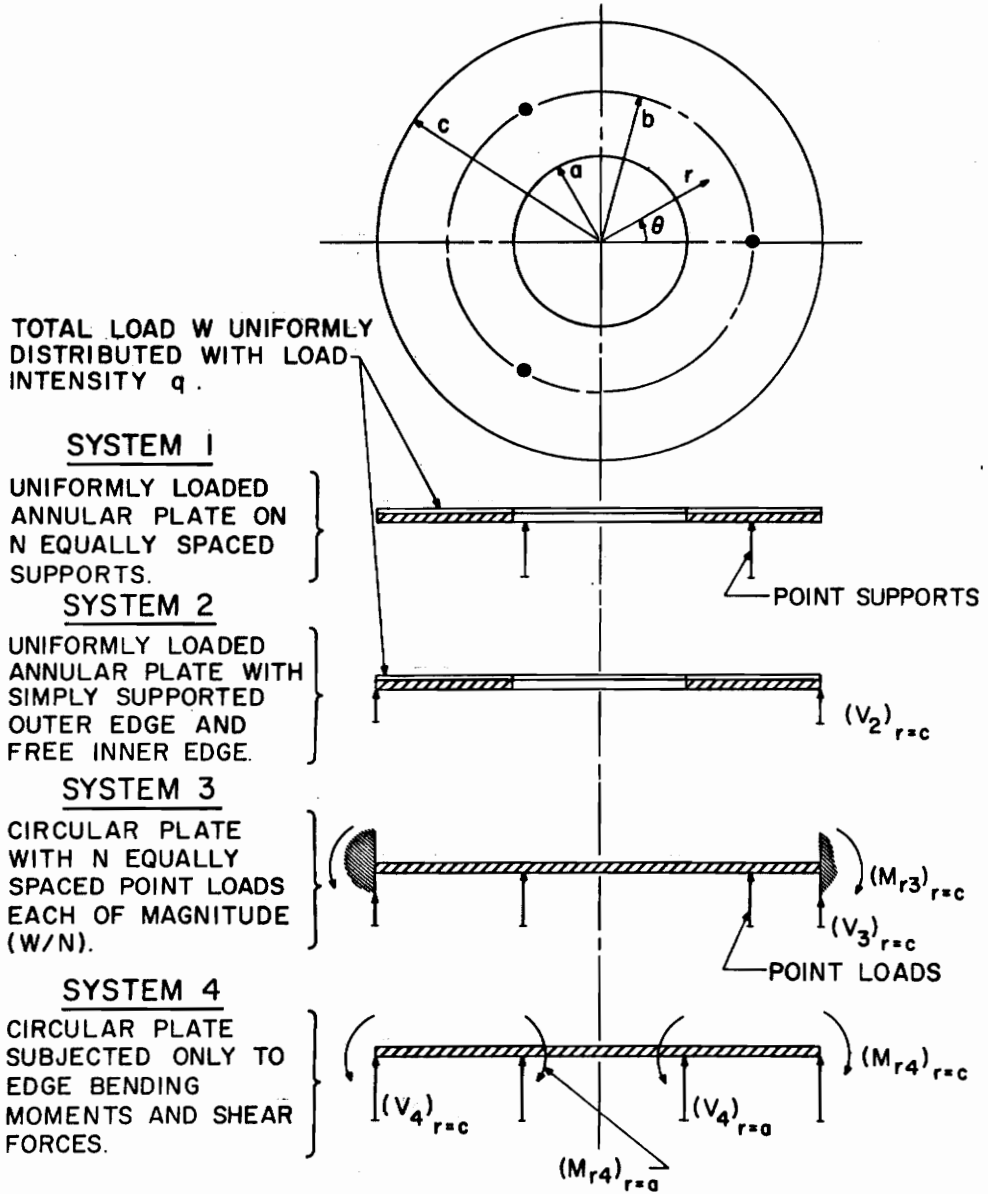


FIG. 17. SCHEMATIC SHOWING SYSTEM I IN RELATION TO SYSTEM 2, 3, AND 4.

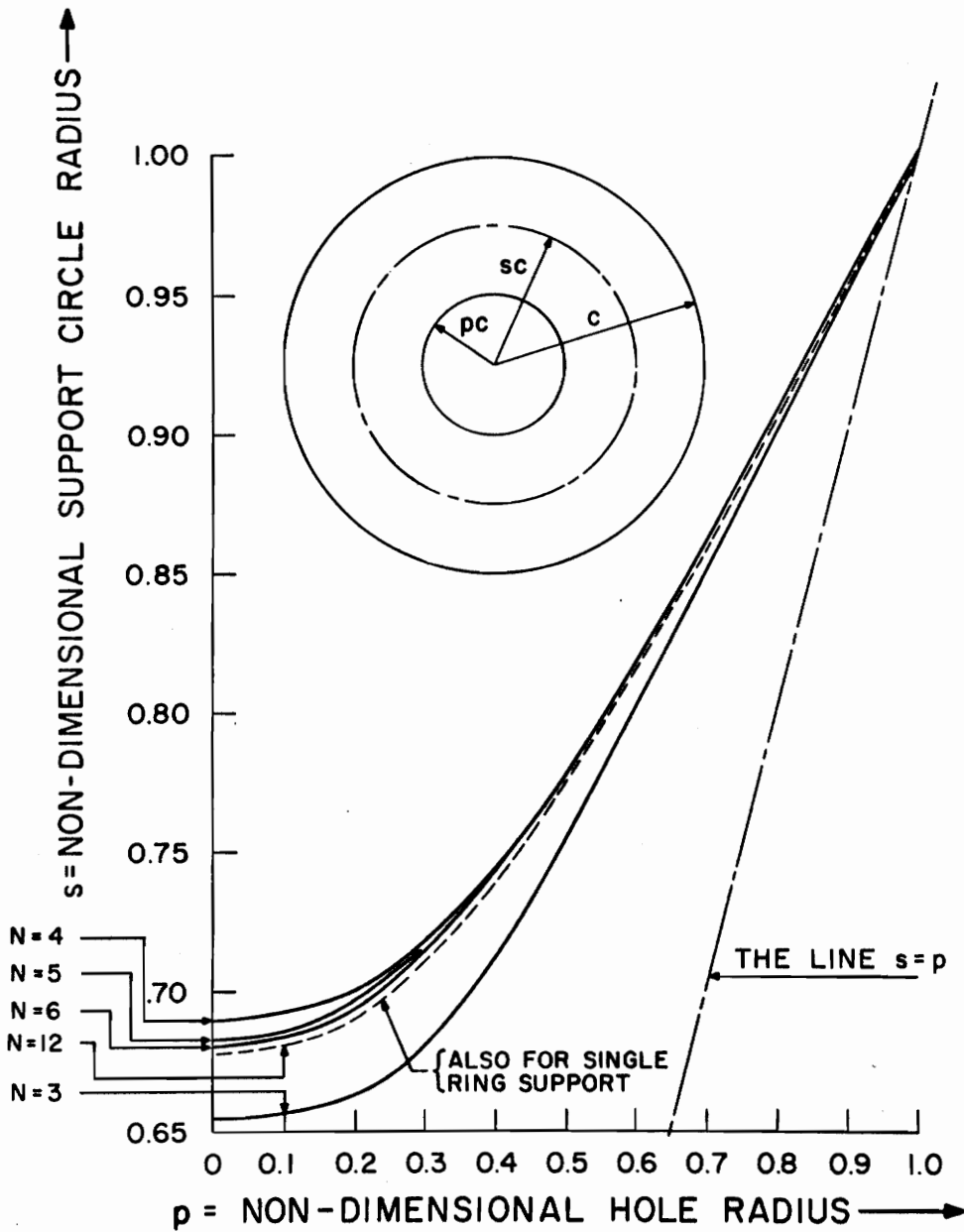


FIG. 18 OPTIMUM POSITION FOR LEAST PEAK-TO-PEAK DEFLECTION FOR A UNIFORMLY LOADED ANNULAR PLATE ON MULTIPOINT SUPPORTS.

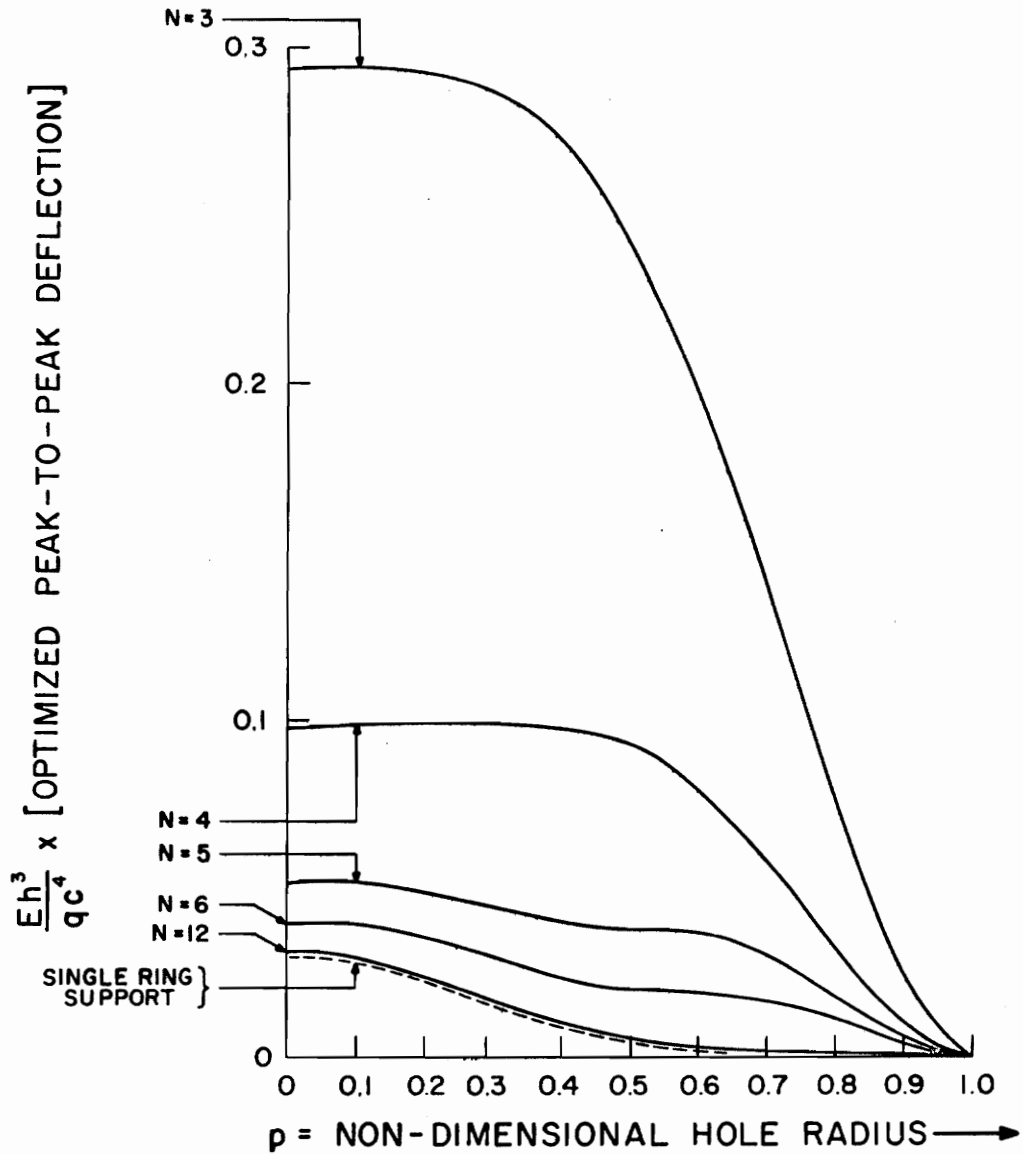


FIG. 19. OPTIMIZED PEAK-TO-PEAK DEFLECTION vs HOLE SIZE, FOR A UNIFORMLY LOADED ANNULAR PLATE ON MULTIPOINT SUPPORTS.

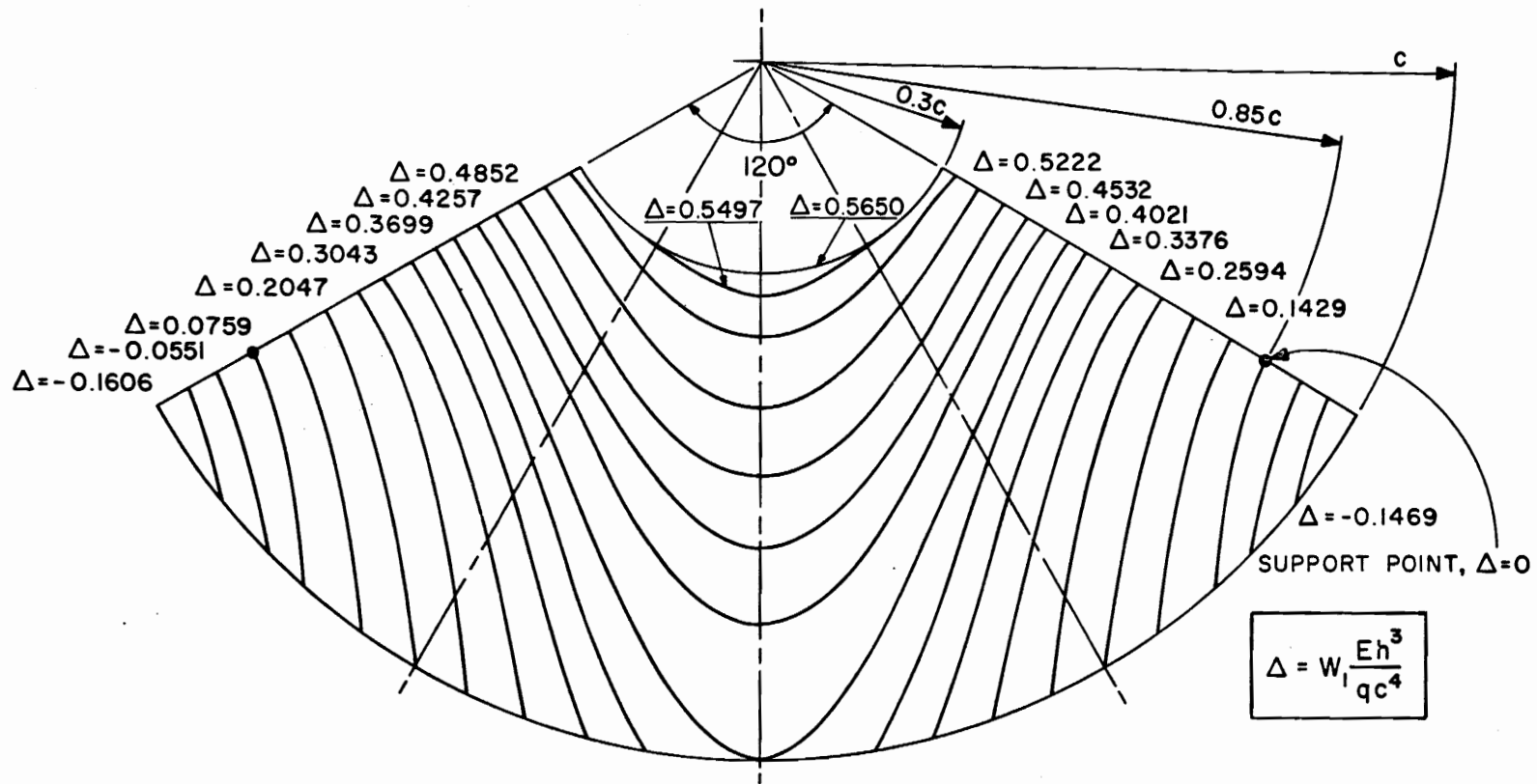


FIG. 20 CONTOUR MAP OF UNIFORMLY LOADED ANNULAR PLATE ON THREE EQUALLY SPACED POINT SUPPORTS WHICH ARE NOT AT THE OPTIMUM POSITIONS.

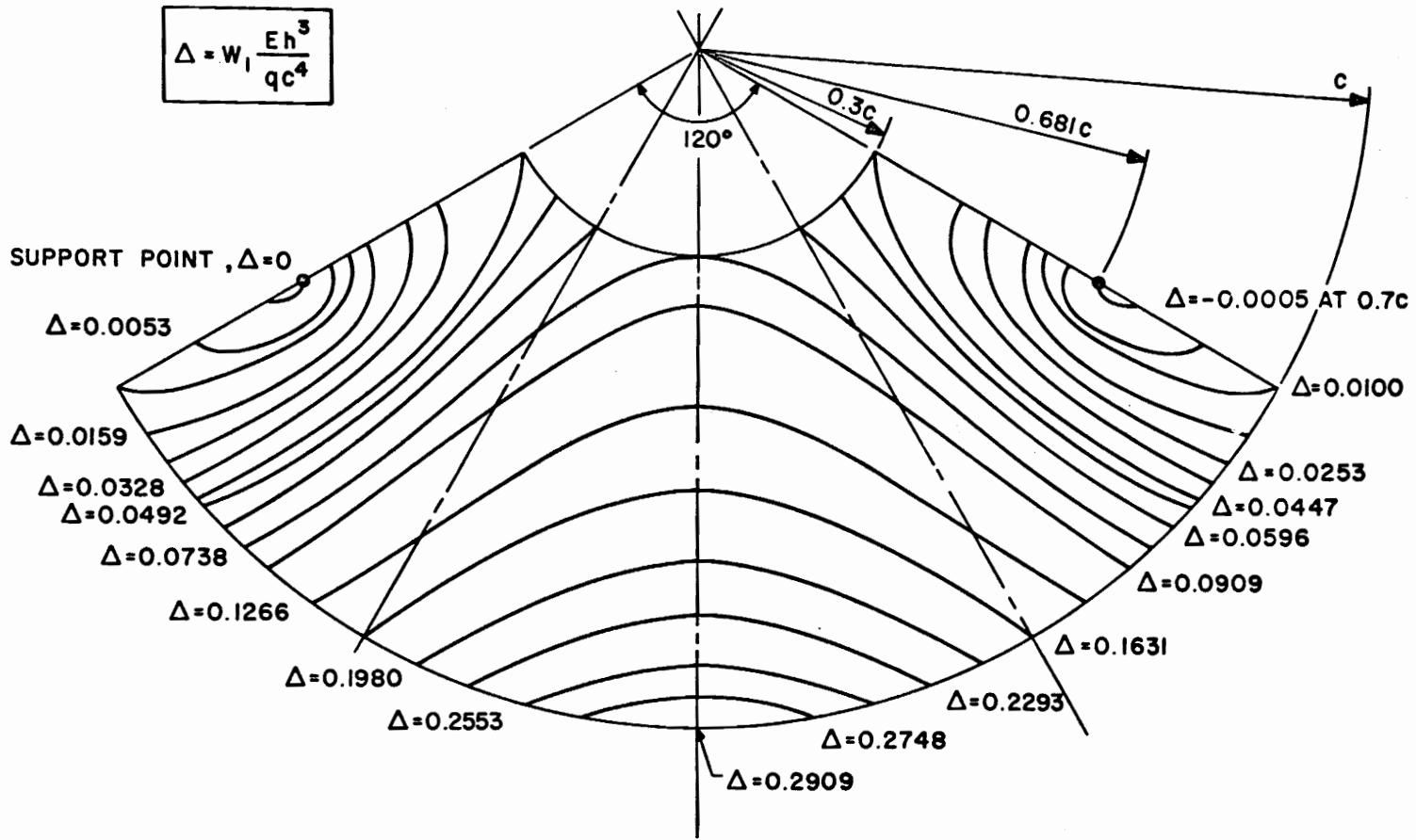


FIG. 21 CONTOUR MAP OF A UNIFORMLY LOADED ANNULAR PLATE WITH THREE EQUALLY SPACED POINT SUPPORTS AT THE OPTIMUM POSITIONS.

NUMBER OF SUPPORTS, N = 3											
POISSON'S RATIO, $\nu = 0.17$						ANGLE $\theta = 0$					
DEFLECTION COEFFICIENT β											
$\frac{x}{s}$	0	0.1	0.2	0.3	0.4	0.5	0.6	0.7	0.8	0.9	1.0
0.1	-0.027370	0	0.080201	0.188926	0.312506	0.443259	0.576281	0.708462	0.838033	0.964304	1.087507
0.2	-0.068665	-0.051202	0	0.090264	0.200871	0.320916	0.444466	0.567903	0.689163	0.807376	0.922659
0.3	-0.099569	-0.087961	-0.055220	0	0.086705	0.188513	0.296118	0.404799	0.511940	0.616360	0.718001
0.4	-0.105003	-0.097783	-0.078015	-0.046696	0	0.072958	0.157217	0.244612	0.331400	0.415854	0.497664
0.5	-0.071502	-0.067911	-0.058851	-0.045769	-0.027923	0	0.050115	0.108511	0.167967	0.225638	0.280705
0.6	0.015179	0.015586	0.015173	0.012309	0.006810	0.000589	0	0.018095	0.041849	0.064926	0.085446
0.7	0.171589	0.169086	0.159929	0.142309	0.115524	0.080304	0.039414	0	-0.024117	-0.045154	-0.068472
0.8	0.418307	0.413065	0.395597	0.363859	0.316720	0.254168	0.177576	0.090291	0	-0.078925	-0.157924
0.9	0.783557	0.775683	0.750157	0.704626	0.637522	0.548187	0.437000	0.305602	0.157423	0	-0.152540
1.0	1.317198	1.306757	1.273313	1.214138	1.127183	1.011126	0.865392	0.690155	0.486295	0.255331	0

NUMBER OF SUPPORTS, $N = 3$											
POISSON'S RATIO, $\nu = 0.17$						ANGLE $\theta = 30^\circ$					
DEFLECTION COEFFICIENT β											
$\frac{x}{s}$	0	0.1	0.2	0.3	0.4	0.5	0.6	0.7	0.8	0.9	1.0
0.1	-0.027370	0.001562	0.081318	0.189714	0.313127	0.443792	0.576774	0.708949	0.838538	0.964846	1.088100
0.2	-0.068665	-0.050085	0.006277	0.095955	0.205557	0.325022	0.448309	0.571724	0.693148	0.811672	0.927376
0.3	-0.099569	-0.087173	-0.049529	0.014389	0.101059	0.201620	0.308618	0.417364	0.525148	0.630684	0.733799
0.4	-0.105003	-0.097162	-0.073329	-0.032342	0.026795	0.101377	0.185387	0.273425	0.362011	0.449317	0.534795
0.5	-0.071502	-0.067378	-0.054746	-0.032667	0.000496	0.045659	0.100949	0.162350	0.226135	0.289933	0.352725
0.6	0.015179	0.016079	0.019017	0.024809	0.034980	0.051424	0.075151	0.105106	0.138814	0.173937	0.209091
0.7	0.171589	0.169572	0.163749	0.154874	0.144337	0.134144	0.126425	0.122452	0.121995	0.123829	0.126745
0.8	0.418307	0.413569	0.399582	0.377066	0.347331	0.312336	0.274541	0.236403	0.199634	0.164818	0.131754
0.9	0.783557	0.776225	0.754454	0.718949	0.670984	0.612481	0.546012	0.474585	0.401165	0.328082	0.256775
1.0	1.317198	1.307350	1.278029	1.229936	1.164334	1.083146	0.989037	0.885372	0.775973	0.664646	0.554748

NUMBER OF SUPPORTS, N = 3											
POISSON'S RATIO, $\nu = 0.17$						ANGLE $\theta = 60^\circ$					
DEFLECTION COEFFICIENT β											
$\frac{x}{s}$	0	0.1	0.2	0.3	0.4	0.5	0.6	0.7	0.8	0.9	1.0
0.1	-0.027370	0.002542	0.082335	0.190480	0.313740	0.444322	0.577266	0.709434	0.839042	0.965387	1.088692
0.2	-0.068665	-0.049067	0.010223	0.100598	0.209843	0.328951	0.452064	0.575493	0.697099	0.815943	0.932069
0.3	-0.099569	-0.086407	-0.044887	0.023531	0.112095	0.213040	0.320210	0.429392	0.537997	0.644728	0.749346
0.4	-0.105003	-0.096548	-0.069043	-0.021307	0.044257	0.122829	0.209307	0.299566	0.390770	0.481299	0.570584
0.5	-0.071502	-0.066848	-0.050816	-0.021243	0.021947	0.076672	0.139675	0.207669	0.278022	0.349003	0.419801
0.6	0.015179	0.016570	0.022771	0.036402	0.058900	0.090149	0.128738	0.172639	0.219866	0.268895	0.318866
0.7	0.171589	0.170058	0.167519	0.166902	0.170478	0.179462	0.193958	0.213248	0.236248	0.261935	0.289646
0.8	0.418307	0.414673	0.403533	0.389915	0.376090	0.364223	0.355593	0.350656	0.349306	0.351206	0.356112
0.9	0.783557	0.776766	0.758725	0.732994	0.702966	0.671552	0.640969	0.612691	0.587554	0.565996	0.548326
1.0	1.317198	1.307943	1.282722	1.245483	1.200123	1.150221	1.098812	1.048273	1.000331	0.956198	0.916689

NUMBER OF SUPPORTS, N = 6											
POISSON'S RATIO, $\nu = 0.17$						ANGLE $\theta = 0$					
DEFLECTION COEFFICIENT β											
$\frac{x}{s}$	0	0.1	0.2	0.3	0.4	0.5	0.6	0.7	0.8	0.9	1.0
0.1	-0.028641	0	0.079997	0.188432	0.311852	0.442520	0.575502	0.707677	0.837267	0.963575	1.086829
0.2	-0.073776	-0.055246	0	0.090319	0.200246	0.319822	0.443154	0.566587	0.688020	0.806548	0.922253
0.3	-0.111335	-0.098949	-0.061819	0	0.087634	0.189011	0.296398	0.405329	0.513203	0.618779	0.721908
0.4	-0.127131	-0.119294	-0.095658	-0.056130	0	0.075765	0.161133	0.249960	0.338956	0.426448	0.511986
0.5	-0.109838	-0.105715	-0.093169	-0.071842	-0.041324	0	0.056589	0.119754	0.184659	0.248985	0.311917
0.6	-0.049190	-0.048291	-0.045397	-0.040014	-0.031514	-0.018999	0	0.030998	0.066488	0.102541	0.137787
0.7	0.064966	0.062947	0.057100	0.047982	0.036377	0.023259	0.010062	0	-0.000558	0.001766	0.003963
0.8	0.243654	0.238916	0.224913	0.202234	0.171752	0.134543	0.091931	0.045821	0	-0.038512	-0.075592
0.9	0.500561	0.493229	0.471445	0.435814	0.387248	0.326873	0.255989	0.176150	0.089492	0	-0.085119
1.0	0.859348	0.849499	0.820167	0.771961	0.705803	0.622823	0.524252	0.411363	0.285462	0.147898	0

NUMBER OF SUPPORTS, N = 6											
POISSON'S RATIO, $\nu = 0.17$						ANGLE $\theta = 15^\circ$					
DEFLECTION COEFFICIENT β											
$\frac{x}{s}$	0	0.1	0.2	0.3	0.4	0.5	0.6	0.7	0.8	0.9	1.0
0.1	-0.028641	0.000181	0.080022	0.188438	0.311854	0.442521	0.575503	0.707678	0.837267	0.963575	1.086829
0.2	-0.073776	-0.055221	0.000726	0.090591	0.200346	0.319866	0.443176	0.566600	0.688029	0.806555	0.922259
0.3	-0.111335	-0.098943	-0.061548	0.001633	0.088523	0.189441	0.296627	0.405464	0.513292	0.618848	0.721971
0.4	-0.127131	-0.119293	-0.095557	-0.055242	0.002904	0.077680	0.162234	0.250638	0.339422	0.426819	0.512326
0.5	-0.109838	-0.105714	-0.093125	-0.071412	-0.039408	0.004555	0.059954	0.121993	0.186263	0.250303	0.313160
0.6	-0.049190	-0.048291	-0.045375	-0.039785	-0.030413	-0.015605	0.006676	0.036513	0.070705	0.106152	0.141311
0.7	0.064966	0.062948	0.057113	0.048116	0.037055	0.025498	0.015577	0.009669	0.008433	0.009979	0.012358
0.8	0.243654	0.238916	0.224921	0.202324	0.172218	0.136147	0.096148	0.054812	0.014863	-0.022451	-0.057902
0.9	0.500561	0.493229	0.471451	0.435884	0.387619	0.328192	0.259599	0.184362	0.105554	0.026345	-0.051331
1.0	0.859348	0.849499	0.820173	0.772023	0.706144	0.624066	0.527775	0.419759	0.303120	0.181686	0.059676

		NUMBER OF SUPPORTS, N = 6										
		POISSON'S RATIO, $\nu = 0.17$						ANGLE $\theta = 30^\circ$				
		DEFLECTION COEFFICIENT β										
$\frac{x}{s}$	0	0.1	0.2	0.3	0.4	0.5	0.6	0.7	0.8	0.9	1.0	
0.1	-0.028641	0.000291	0.080047	0.188443	0.311856	0.442522	0.575503	0.707678	0.837267	0.963575	1.086829	
0.2	-0.073776	-0.055196	0.001166	0.090844	0.200445	0.319911	0.443198	0.566612	0.688037	0.806561	0.922265	
0.3	-0.111335	-0.098938	-0.061295	0.002623	0.089294	0.189855	0.296852	0.405598	0.513382	0.618918	0.722033	
0.4	-0.127131	-0.119291	-0.095458	-0.054471	0.004666	0.079249	0.163258	0.251296	0.339883	0.427188	0.512666	
0.5	-0.109838	-0.105713	-0.093081	-0.070998	-0.037839	0.007324	0.062614	0.124015	0.187799	0.251597	0.314389	
0.6	-0.049190	-0.048291	-0.045352	-0.039559	-0.029389	-0.012945	0.010782	0.040737	0.074445	0.109568	0.144722	
0.7	0.064966	0.062948	0.057125	0.048249	0.037713	0.027519	0.019801	0.015828	0.015371	0.017206	0.020121	
0.8	0.243654	0.238916	0.224929	0.202413	0.172678	0.137683	0.099888	0.061750	0.024982	-0.009835	-0.042899	
0.9	0.500561	0.493229	0.471458	0.435953	0.387988	0.329485	0.263015	0.191589	0.118169	0.045085	-0.026229	
1.0	0.859348	0.849499	0.820179	0.772086	0.706483	0.625295	0.531186	0.427522	0.318123	0.206788	0.096759	

NUMBER OF SUPPORTS, N = 9											
POISSON'S RATIO, $\nu = 0.17$						ANGLE $\theta = 0$					
DEFLECTION COEFFICIENT β											
$\frac{x}{s}$	0	0.1	0.2	0.3	0.4	0.5	0.6	0.7	0.8	0.9	1.0
0.1	-0.028759	0	0.079903	0.188320	0.311736	0.442403	0.575385	0.707560	0.837149	0.963457	1.086711
0.2	-0.074246	-0.055692	0	0.090086	0.199871	0.319395	0.442706	0.566129	0.687558	0.806084	0.921789
0.3	-0.112393	-0.100002	-0.062641	0	0.087299	0.188342	0.295557	0.404402	0.512233	0.617789	0.720912
0.4	-0.129014	-0.121175	-0.097445	-0.057289	0	0.075371	0.160209	0.248703	0.337517	0.424925	0.510436
0.5	-0.112795	-0.108672	-0.096084	-0.074410	-0.042792	0	0.056162	0.118692	0.183152	0.247263	0.310144
0.6	-0.053564	-0.052665	-0.049749	-0.044171	-0.034929	-0.020813	0	0.030739	0.065639	0.101386	0.136645
0.7	0.058467	0.056449	0.050614	0.041613	0.030503	0.018656	0.007679	0	-0.000273	0.002089	0.004746
0.8	0.233231	0.228493	0.214497	0.191898	0.161772	0.125570	0.085033	0.042181	0	-0.036683	-0.071792
0.9	0.481698	0.474366	0.452588	0.417019	0.368744	0.309246	0.240344	0.164108	0.082881	0	-0.079301
1.0	0.820155	0.810306	0.780979	0.732829	0.666942	0.584813	0.488289	0.379451	0.260459	0.133386	0

NUMBER OF SUPPORTS, N = 9											
POISSON'S RATIO, $\nu = 0.17$						ANGLE $\theta = 10^\circ$					
DEFLECTION COEFFICIENT β											
$\frac{x}{s}$	0	0.1	0.2	0.3	0.4	0.5	0.6	0.7	0.8	0.9	1.0
0.1	-0.028759	0.000053	0.079905	0.188320	0.311736	0.442403	0.575385	0.707560	0.837149	0.963457	1.086711
0.2	-0.074246	-0.055691	0.000212	0.090116	0.199876	0.319396	0.442706	0.566129	0.687558	0.806084	0.921789
0.3	-0.112393	-0.100002	-0.062610	0.000478	0.087438	0.188379	0.295568	0.404406	0.512234	0.617790	0.720913
0.4	-0.129014	0.121175	-0.097440	-0.057152	0.000849	0.075721	0.160333	0.248751	0.337538	0.424936	0.510444
0.5	-0.112795	-0.108672	-0.096083	-0.074373	-0.042442	0.001327	0.056841	0.118984	0.183288	0.247339	0.310199
0.6	-0.053564	-0.052665	-0.049748	-0.044159	-0.034805	-0.020134	0.001914	0.031876	0.066221	0.101731	0.136909
0.7	0.058467	0.056449	0.050614	0.041617	0.030551	0.018948	0.008815	0.002639	0.001527	0.003256	0.005709
0.8	0.233231	0.228493	0.214498	0.191900	0.161793	0.125707	0.085615	0.043981	0.003707	-0.033559	-0.068917
0.9	0.481698	0.474366	0.452588	0.417021	0.368756	0.309323	0.240689	0.165275	0.086006	0.006210	-0.071886
1.0	0.820155	0.810306	0.780979	0.732829	0.666949	0.584869	0.488554	0.380415	0.263334	0.140801	0.016998

NUMBER OF SUPPORTS, N = 9											
POISSON'S RATIO, $\nu = 0.17$						ANGLE $\theta = 20^\circ$					
DEFLECTION COEFFICIENT β											
$\frac{x}{s}$	0	0.1	0.2	0.3	0.4	0.5	0.6	0.7	0.8	0.9	1.0
0.1	-0.028759	0.000085	0.079906	0.188320	0.311736	0.442403	0.575385	0.707560	0.837149	0.963457	1.086711
0.2	-0.074246	-0.055689	0.000340	0.090147	0.199881	0.319397	0.442706	0.566129	0.687558	0.806084	0.921789
0.3	-0.112393	-0.100002	-0.062580	0.000766	0.087567	0.188415	0.295579	0.404410	0.512236	0.617791	0.720913
0.4	-0.129014	0.121175	-0.097435	-0.057022	0.001361	0.076035	0.160454	0.248798	0.337559	0.424947	0.510451
0.5	-0.112795	-0.108672	-0.096082	-0.074338	-0.042129	0.002127	0.057422	0.119265	0.183423	0.247416	0.310255
0.6	-0.053564	-0.052665	-0.049748	-0.044148	-0.034685	-0.019553	0.003069	0.032813	0.066769	0.102070	0.137172
0.7	0.058467	0.056449	0.050614	0.041622	0.030599	0.019229	0.009752	0.004244	0.002979	0.004343	0.006644
0.8	0.233231	0.228493	0.214498	0.191902	0.161815	0.125842	0.086163	0.045434	0.006059	-0.031011	-0.066295
0.9	0.481698	0.474366	0.452588	0.417022	0.368767	0.309399	0.241028	0.166363	0.088553	0.010513	-0.066029
1.0	0.820155	0.810306	0.780979	0.732830	0.666958	0.584924	0.488170	0.381349	0.265956	0.146657	0.027428

NUMBER OF SUPPORTS, N = 15											
POISSON'S RATIO, $\nu = 0.17$						ANGLE $\theta = 0$					
DEFLECTION COEFFICIENT β											
$\frac{x}{s}$	0	0.1	0.2	0.3	0.4	0.5	0.6	0.7	0.8	0.9	1.0
0.1	-0.028797	0	0.079867	0.188282	0.311698	0.442365	0.575347	0.707522	0.837111	0.963419	1.086673
0.2	-0.074399	-0.055843	0	0.089963	0.199723	0.319244	0.442553	0.565977	0.687406	0.805932	0.921636
0.3	-0.112736	-0.100345	-0.062955	0	0.087085	0.188035	0.295225	0.404063	0.511891	0.617447	0.720569
0.4	-0.129624	-0.121785	-0.098050	-0.057771	0	0.075075	0.159719	0.248139	0.336928	0.424326	0.509833
0.5	-0.113749	-0.109625	-0.097037	-0.075328	-0.043432	0	0.055799	0.118015	0.182332	0.246385	0.309245
0.6	-0.054940	-0.054041	-0.051125	-0.045536	-0.036186	-0.021599	0	0.030328	0.064806	0.100345	0.135529
0.7	0.056561	0.054543	0.048708	0.039711	0.028644	0.017027	0.006737	0	-0.000669	0.001263	0.003764
0.8	0.230489	0.225751	0.211756	0.189158	0.159051	0.122962	0.082834	0.040949	0	-0.036781	-0.071917
0.9	0.476890	0.469558	0.447781	0.412213	0.363948	0.304514	0.235872	0.160381	0.080718	0	-0.077969
1.0	0.807848	0.797999	0.768673	0.720523	0.654643	0.572562	0.476243	0.368069	0.250769	0.127218	0

NUMBER OF SUPPORTS, N = 15											
POISSON'S RATIO, $\nu = 0.17$						ANGLE $\theta = 6^\circ$					
DEFLECTION COEFFICIENT β											
$\frac{x}{s}$	0	0.1	0.2	0.3	0.4	0.5	0.6	0.7	0.8	0.9	1.0
0.1	-0.028797	0.000011	0.079867	0.188282	0.311698	0.442365	0.575347	0.707522	0.837111	0.963419	1.086673
0.2	-0.074399	0.055843	0.000040	0.089964	0.199723	0.319244	0.442553	0.565977	0.687406	0.805932	0.921636
0.3	-0.112736	-0.100345	-0.062954	0.000103	0.087092	0.188036	0.295225	0.404063	0.511891	0.617447	0.720569
0.4	-0.129624	-0.121785	-0.098050	-0.057764	0.000182	0.075102	0.159722	0.248140	0.336928	0.424326	0.509833
0.5	-0.113749	-0.109625	-0.097037	-0.075327	-0.043405	0.000285	0.055864	0.118028	0.182334	0.246386	0.309246
0.6	-0.054940	-0.054041	-0.051125	-0.045536	-0.036182	-0.021533	0.000410	0.030453	0.064837	0.100354	0.135533
0.7	0.056561	0.054543	0.048708	0.039711	0.028645	0.017039	0.006862	0.000558	-0.000459	0.001330	0.003795
0.8	0.230489	0.225751	0.211756	0.189158	0.159051	0.122965	0.082864	0.041159	0.000737	-0.036431	-0.071721
0.9	0.476890	0.469558	0.447781	0.412213	0.363948	0.304515	0.235880	0.160448	0.081068	0.001067	-0.077043
1.0	0.807848	0.797999	0.768673	0.720523	0.654643	0.572562	0.476247	0.368101	0.250965	0.128144	0.003569

NUMBER OF SUPPORTS, N = 15											
POISSON'S RATIO, $\nu = 0.17$						ANGLE $\theta = 12^\circ$					
DEFLECTION COEFFICIENT β											
$\frac{x}{s}$	0	0.1	0.2	0.3	0.4	0.5	0.6	0.7	0.8	0.9	1.0
0.1	-0.028797	0.000018	0.079867	0.188282	0.311698	0.442365	0.575347	0.707522	0.837111	0.963419	1.086673
0.2	-0.074399	-0.055843	0.000073	0.089964	0.199723	0.319244	0.442553	0.565977	0.687406	0.805932	0.921636
0.3	-0.112736	-0.100345	-0.062953	0.000164	0.087099	0.188036	0.295225	0.404063	0.511891	0.617447	0.720569
0.4	-0.129624	-0.121785	-0.098050	-0.057756	0.000292	0.075129	0.159726	0.248141	0.336928	0.424326	0.509833
0.5	-0.113749	-0.109625	-0.097037	-0.075327	-0.043378	0.000456	0.055926	0.118039	0.182337	0.246386	0.309246
0.6	-0.054941	-0.054041	-0.051125	-0.045536	-0.036179	-0.021471	0.000656	0.030569	0.064867	0.100362	0.135536
0.7	0.056561	0.054543	0.048708	0.039711	0.028645	0.017051	0.006977	0.000894	-0.000271	0.001395	0.003827
0.8	0.230489	0.225751	0.211756	0.189158	0.159052	0.122967	0.082895	0.041348	0.001182	-0.036123	-0.071530
0.9	0.476890	0.469558	0.447781	0.412213	0.363948	0.304516	0.235889	0.160513	0.081375	0.001760	-0.076237
1.0	0.807848	0.797999	0.768673	0.720523	0.654643	0.572562	0.476251	0.368132	0.251156	0.128950	0.005740

APPENDIX A

SYSTEM 2. System 2 is defined to be, a simply supported circular plate of radius c subjected to a total load W symmetrically distributed with respect to the centre of the plate. If the transverse deflections of the plate are denoted by w_2 , then the deflections are related to the load intensity $q(r)$ by,

$$\nabla^4 w_2 = \frac{1}{r} \frac{d}{dr} \left\{ r \frac{d}{dr} \left[\frac{1}{r} \frac{d}{dr} \left(r \frac{dw_2}{dr} \right) \right] \right\} = \frac{q(r)}{D} \quad (A1)$$

where, D is the flexural rigidity and $q(r)$ related to W by (2).

As the plate is symmetrically loaded and simply supported, it follows that, the edge radial bending moment $(M_{r2})_{r=c}$ and the edge reaction $(V_2)_{r=c}$ are given by the following expressions

$$(M_{r2})_{r=c} = -D \left[\nu \nabla^2 w_2 + \frac{(1-\nu)}{c^2} \frac{\partial^2 w_2}{\partial x^2} \right]_{x=1} = 0 \quad (A2)$$

$$(V_1)_{r=c} = -D \left[\frac{1}{c} \frac{\partial \nabla^2 w_2}{\partial x} + \frac{(1-\nu)}{\partial c^3 x} \frac{\partial^2}{\partial x \partial \theta} \left[\frac{1}{x} \frac{\partial w_2}{\partial \theta} \right] \right]_{x=1} = -\frac{W}{2\pi c} \quad (A3)$$

where, x and ∇^2 are defined by equation (6).

SYSTEM 3. System 3 is defined to be, a clamped circular plate of radius c subjected to N concentrated forces, each of magnitude (W/N) , and situated equal distance apart on a single concentric circle of radius b . The deflections w_3 corresponding to this system will now be obtained by extending the work of Michell (4). The deflection surface w corresponding to a circular plate of radius c carrying one eccentric force $(-W/N)$ at $r=b$ and $\theta=0$, is given by Michell and quoted in page 293 of Reference (14), as

$$W = \frac{Wc^2}{16\pi ND} \left\{ (x^2-1)(1-s^2) + (x^2+s^2-2xs \cos\theta) \log \left[\frac{1+x^2s^2-2xs \cos\theta}{x^2+s^2-2xs \cos\theta} \right] \right\} \quad (A4)$$

where, x is defined by (6) and s is the ratio,

$$s = b/c \quad (A5)$$

Suppose that on the circle of radius $r=b$ there are N concentrated forces, each of value $(-W/N)$ and placed at equal distances apart; then by applying the principle of superposition, the deflections w_3 due to these forces are

$$w_3 = \frac{Wc^2}{16\pi D} \left[(x^2-1)(1-s^2) + \frac{1}{N} \sum_{n=1}^N [x^2+s^2-2xs \cos(\theta-n\alpha)] \log \left[\frac{1+x^2s^2-2xs \cos(\theta-n\alpha)}{x^2+s^2-2xs \cos(\theta-n\alpha)} \right] \right] \quad (A6)$$

where, $\alpha = 2\pi/N$

It can be verified that w_3 is a biharmonic function. The edge bending moment and the edge reaction for this system are respectively

$$\begin{aligned} (M_{r3})_{r=c} &= -D \left[\nu \nabla^2 w_3 + \frac{(1-\nu)}{c^2} \frac{\partial^2 w_3}{\partial x^2} \right]_{x=1} \\ &= \frac{W}{4\pi N} \sum_{n=1}^N \frac{(1-s^2)^2}{[1+s^2-2s \cos(\theta-n\alpha)]} \\ &= \frac{W(1-s^2)}{4\pi} + \frac{W(1-s^2)}{2\pi N} \sum_{n=1}^N \sum_{m=2}^{\infty} s^m \cos m(\theta-n\alpha) \end{aligned} \quad (A7)$$

$$\begin{aligned}
(V_3)_{r=c} &= -D \left[\frac{1}{c} \frac{\partial^2 w_3}{\partial x^2} + \frac{(1-\nu)}{c^3 x} \frac{\partial^2}{\partial x \partial \theta} \left[\frac{1}{x} \frac{\partial w_3}{\partial \theta} \right] \right]_{x=1} \\
&= \frac{W}{4\pi Nc} \sum_{n=1}^N \frac{(1-s^2)^3}{[1 + s^2 - 2s \cos(\theta - n\alpha)]^2} \\
&\quad + \frac{W}{4\pi Nc} \sum_{n=1}^N \frac{(1-s^2)^2}{[1 + s^2 - 2s \cos(\theta - n\alpha)]} \\
&= \frac{W}{2\pi c} \left[1 + \frac{1}{N} \sum_{n=1}^N \sum_{m=2}^{\infty} [2 + m(1-s^2)] s^m \cos m(\theta - n\alpha) \right] \quad (A8)
\end{aligned}$$

APPENDIX B

For $\alpha = 2\pi/N$

$$\sum_{n=1}^N \cos m(\theta - n\alpha) = \begin{cases} N \cos m\theta & \text{if } m \text{ is a multiple of } N \\ 0 & \text{if } m \text{ is not a multiple of } N \end{cases} \quad (\text{B1})$$

From Reference (28), page 41, for $p^2 \leq 1$

$$\sum_{n=1}^N \log [1 + p^2 - 2p \cos (\theta - n\alpha)] = -2 \sum_{n=1}^N \sum_{m=1}^{\infty} \frac{p^m \cos m(\theta - n\alpha)}{m} \quad (\text{B2})$$

Since the number of supports N is greater than or equal to 2, it follows from equation (B1) that

$$\sum_{n=1}^N \cos(\theta - n\alpha) = 0 \quad (\text{B3})$$

substituting $p=xs$ in equation (B2) and using equation (B3) gives,

$$\sum_{n=1}^N \log [1+x^2s^2-2xs \cos(\theta-n\alpha)] = -2 \sum_{n=1}^N \sum_{m=2}^{\infty} \frac{x^m s^m \cos m(\theta-n\alpha)}{m} \quad (\text{B4})$$

By means of Fourier series and use of the integrals (6) and (8) in page 593 of Reference (28), it can be shown that,

$$\begin{aligned} Nx^2s^2 + \sum_{n=1}^N xs \cos(\theta-n\alpha) \log [1+x^2s^2-2xs \cos(\theta-n\alpha)] \\ = - \sum_{n=1}^N \sum_{m=2}^{\infty} \left[\frac{1}{m-1} + \frac{x^2s^2}{m+1} \right] x^m s^m \cos m(\theta-n\alpha) \end{aligned} \quad (\text{B5})$$

By substituting $s=1$ in equation (B4) and (B5) it can be established that

$$\sum_{n=1}^N [1 + x^2 - 2x \cos(\theta - n\alpha)] \log [1 + s^2 - 2x \cos(\theta - n\alpha)]$$

$$= 2Nx^2 + 2 \sum_{n=1}^N \sum_{m=2}^{\infty} \left[\frac{1}{m(m-1)} - \frac{x^2}{m(m+1)} \right] x^m \cos m(\theta - n\alpha) \quad (B6)$$

$$= 2Nx^2 + 2N \sum_{m=N, 2N, \dots}^{\infty} \left[\frac{1}{m(m-1)} - \frac{x^2}{m(m+1)} \right] x^m \cos m\theta \quad (B7)$$

substituting $x=1$ and $\theta=0$ in equation (B7) yields

$$\sum_{n=1}^N (1 - \cos n\alpha) \log [2(1 - \cos n\alpha)] = N + 2N \sum_{m=N, 2N, \dots}^{\infty} \frac{1}{m(m^2 - 1)} \quad (B8)$$

Consider the function $L(\zeta_n)$

where,

$$\left. \begin{aligned} \zeta_n &= xs e^{-i(\theta - n\alpha)} \\ \text{and} \\ L(\zeta_n) &= \sum_{m=2}^{\infty} \frac{\zeta_n^m}{m^2(m-1)} \end{aligned} \right\} \quad (B9)$$

Denoting the real part of $L(\zeta_n)$ by $R_e L(\zeta_n)$,

$$R_e L(\zeta_n) = \sum_{m=2}^{\infty} \frac{x^m s^m}{m^2(m-1)} \cos m(\theta - n\alpha)$$

$$= R_e \left[\sum_{m=2}^{\infty} \left[\frac{1}{m-1} - \frac{1}{m} - \frac{1}{2m} \right] \zeta_n^m \right]$$

$$= R_e \left\{ \left[\sum_{m=2}^{\infty} \zeta_n \frac{\zeta_n^{m-1}}{m-1} \right] - \left[\sum_{m=2}^{\infty} \frac{\zeta_n^m}{m} \right] - \Omega(\zeta_n) \right\} \quad (B10)$$

where,

$$\Omega(\zeta_n) = \sum_{m=2}^{\infty} \frac{\zeta_n^m}{m}$$

and

$$R_e \Omega(\zeta_n) = \sum_{m=2}^{\infty} \frac{x^m s^m}{m^2} \cos m(\theta - n\alpha) \quad (\text{B12})$$

since

$$\sum_{m=2}^{\infty} \frac{\zeta_n^{m-1}}{m-1} = \sum_{m=1}^{\infty} \frac{\zeta_n^m}{m} = -\log(1 - \zeta_n) \quad (\text{B13})$$

it follows that the equation (B10) can be written as

$$\sum_{m=2}^{\infty} \frac{x^m s^m}{m^2(m-1)} \cos m(\theta - n\alpha) = R_e [(1 - \zeta_n) \log(1 - \zeta_n) + \zeta_n] - R_e \Omega(\zeta_n)$$

Summing both sides of the above equation from $n=1$ to $n=N$ yields,

$$\sum_{n=1}^N \sum_{m=2}^{\infty} \frac{x^m s^m}{m^2(m-1)} \cos m(\theta - n\alpha) = R_e \left[\sum_{n=1}^N (1 - \zeta_n) \log(1 - \zeta_n) \right] - R_e \left[\sum_{n=1}^N \Omega(\zeta_n) \right] \quad (\text{B14})$$

In the particular case when $x=s$ and $\theta=0$, equation (B14) reduces to

$$\begin{aligned} \sum_{n=1}^N \sum_{m=2}^{\infty} \frac{s^{2m}}{m^2(m-1)} = \cos m\alpha = R \left[\sum_{n=1}^N (1 - s^2 e^{-in\alpha}) \log(1 - s^2 e^{-in\alpha}) \right] \\ - \sum_{n=1}^N \sum_{m=2}^{\infty} \frac{s^{2m}}{m} \cos m\alpha \end{aligned} \quad (\text{B15})$$

Using equation (B1), the above equation can be written as,

$$\begin{aligned} \sum_{m=N, 2N, \dots}^{\infty} \frac{s^{2m}}{m^2(m-1)} = \frac{1}{2} \sum_{n=1}^N (1 - s^2 \cos n\alpha) \log(1 + s^4 - 2s^2 \cos n\alpha) \\ - \sum_{n=1}^{N-1} s^2 \Psi(s) \sin n\alpha - \frac{1}{N} \sum_{n=1}^{\infty} \frac{s^{2Nm}}{m^2} \end{aligned} \quad (\text{B16})$$

where,

$$\Psi(s) = \tan^{-1} \left(\frac{s^2 \sin n\alpha}{1 - s^2 \cos n\alpha} \right) \quad (\text{B17})$$

substituting $s=1$ in equation (B16) gives,

$$\sum_{m=N,2N,\dots}^{\infty} \frac{1}{m^2(m-1)} = \frac{1}{2N} \sum_{n=1}^{N-1} (1 - \cos n\alpha) \log [2(1 - \cos n\alpha)]$$

$$- \frac{1}{N} \sum_{n=1}^{N-1} \psi(1) \sin n\alpha - \frac{1}{N^2} \sum_{m=1}^{\infty} \frac{1}{m} \quad (\text{B18})$$

since,

$$(1 - \cos n\alpha) = 2 \sin^2 n\alpha/2 \quad (\text{B19})$$

and from equation (B17)

$$\psi(1) = \tan^{-1} \left(\frac{\sin n\alpha}{1 - \cos n\alpha} \right) = \tan^{-1} (\cot n\alpha/2)$$

$$= (\pi - n\alpha)/2 \quad (\text{B20})$$

and from Reference (29), page 67,

$$\sum_{m=1}^{\infty} \frac{1}{m^2} = \frac{\pi^2}{6} \quad (\text{B21})$$

therefore using equations (B19), (B20) and (B21) equation (B18) becomes,

$$\sum_{m=N,2N,\dots}^{\infty} \frac{1}{m^2(m-1)} = \frac{2}{N} \sum_{n=1}^{N-1} \sin^2 \frac{n\alpha}{2} \log (2 \sin n\alpha/2)$$

$$- \frac{1}{2N} \sum_{n=1}^{N-1} (\pi - n\alpha) \sin n\alpha - \frac{\pi^2}{6N^2} \quad (\text{B22})$$

VITA

The author was born on January 3, 1940, in Singapore. He received his secondary and high school education in England. During the period 1956-1963 he was an engineering apprentice with English Electric Company, Rugby, England, and through a cooperative program attended Rugby College of Technology and gained a diploma in Mechanical Engineering. From 1963 to 1966 he was a full-time student at the University of Hull, England, and obtained a B.Sc. (Hon.) degree in Pure and Applied Mathematics. After graduation from the University of Hull, England, he was employed by English Electric Company in their steam turbine division as a stress analyst. Since the summer of 1967 he has been a resident of U.S.A. and until September, 1972, he was an employee of Lockheed Aircraft Corporation, Science and Engineering Division.

R. Williams.

ABSTRACT

Analytical expressions for the deflection surface of symmetrically loaded circular and annular plates resting on discrete point supports are derived. The formulation of the problem is based on classical small deflection plate theory. It is also assumed, in the formulation, that the supports are situated equal distances apart on a single concentric circle. There is no restriction placed on the number of supports or on the size of the support circle which could be as large as the plate itself or as small as the size of the hole of the annular plate.

The singularity effects associated with the concentrated supports on the plate problems considered here are accounted for in the solution, by drawing an analogy from the Michell's solution to a clamped circular plate subjected to an eccentric point load. This procedure yields solutions in much more suitable form for practical numerical problems than other known methods.

In the case of circular plates on multipoint supports, explicit solutions are given to a number of loading conditions. Solutions to a uniformly loaded circular plate on multipoint supports are compared with the published experimental results; the conclusions are favorable. From the numerical data obtained for a uniformly loaded circular plate on multipoint supports, a procedure is outlined for obtaining contour maps of deformed uniformly loaded plates with discrete supports on two support circles.

Solutions to annular plates on multipoint supports are derived for

the first time. By utilizing this result, design charts are drawn to indicate the optimum size of the support circle, which would produce least peak-to-peak displacements for any given size of hole, and a specified number of supports. Contour maps associated with annular plates on three point supports are also drawn to illustrate the influence of support circle on the displacements. It was found that when there are a fewer number of supports and/or the size of the hole is small, the magnitude of peak-to-peak displacements and the size of the optimum support circle are considerably different from the associated quantities when the support is a continuous ring.